NTNU – Trondheim
Norwegian University of
Science and Technology

Master Project

Bidirectional Control

A Radiating Plantwide Control Method for Maximizing Throughput

Author:
Brage Bang
Supervisor:
Sigurd Skogestad

December 31, 2024

Abstract

This thesis examines the application of bidirectional control in managing non-linear systems, focusing on distillation columns and the ethylbenzene production process. Bidirectional control effectively addresses bottlenecks and distributes throughput manipulations (TPM) dynamically, ensuring consistent operation.

For distillation processes, proportional adjustments to reboiler duty, reflux, and feed-forward ratios stabilize the system, achieving near-total disturbance rejection when properly tuned. A balance between tight and loose control is essential: tight control manages dynamic variables like temperature, while loose control optimizes inventory buffering and economic performance.

Key contributions include introducing adaptive tuning parameters, Δu_T^* and Δy_S^*, to enhance stability and responsiveness. The concept of "multidirectional control," similar to model predictive control (MPC), is also proposed as a potential enhancement to parallelize bottleneck management and further optimize system efficiency.

This approach has broader potential in industries such as wastewater and municipal water management, where robust inventory control and throughput optimization are critical. Proper tuning of control parameters enables efficient, adaptable, and stable operation under varying conditions.

Sammendrag

Denne oppgaven undersøker anvendelsen av "bidireksjonal kontroll" for å håndtere ikke-lineære systemer, med fokus på destillasjonskolonner og etylbenzenproduksjon. Bidireksjonal kontroll håndterer flaskehalser effektivt og flytter strømningsmanipulatoren (TPM) dynamisk, noe som sikrer konsistent drift.

For destillasjonsprosesser stabiliseres systemet ved proporsjonale justeringer av oppkok, tilbakeløp og feed-forward-forhold, noe som muliggjør nesten fullstendig forstyrrelsesavvergelse når kontrollen er riktig justert. En balanse mellom streng og fleksibel kontroll er avgjørende: Streng kontroll håndterer dynamiske variabler som temperatur, mens fleksibel kontroll optimerer buffere og økonomisk ytelse.

Hovedbidragene inkluderer introduksjonen av adaptive justeringsparametere, Δu_T^* og Δy_S^*, for å forbedre stabilitet og respons. Konseptet "multidireksjonal kontroll," lignende modellprediktiv kontroll (MPC), foreslås også som en potensiell forbedring for å parallellisere flaskehalsstyring og optimalisere systemets effektivitet ytterligere.

Denne tilnærmingen har bred anvendelsespotensial i industrier som avløpsvannbehandling og kommunal vannforsyning, hvor robust lagerstyring og optimalisering av gjennomstrømning er kritisk. Riktig innstilling av kontrollparametere muliggjør effektiv, tilpasningsdyktig og stabil drift under varierende forhold.

Foreword

This thesis is my Master of Science (Sivilingeniør) at the *Norwegian University of Science and Technology* (NTNU).

The journey of completing this thesis has been both challenging and rewarding, and I am deeply grateful to the people who have supported me throughout this process.

First and foremost, I would like to extend my heartfelt thanks to Aayush Gupta and his team for providing the steady-state ethylbenzene plant model in Aspen. Your invaluable assistance laid the foundation for this research, and without your help, much of this work would not have been possible.

I am also immensely thankful to my parents, who not only supported me emotionally but also ensured I was well-fed and cared for during this demanding period. Your unwavering encouragement means the world to me.

To my friends, thank you for being my constant source of motivation and companionship. A special thanks to Ellen, whose relentless nudging always brought me back to focus and reminded me of the importance of perseverance.

Finally, I want to express my gratitude to my supervisor, Sigurd Skogestad, for your guidance, insights, and patience. Your expertise and constructive feedback have been invaluable in shaping this work.

This thesis is a culmination of the contributions, patience, and encouragement from all of you. I am truly grateful.

Process regulation has been and is a joy. Now, I will move on to regulation of rocket engines!

Brage Bang Trondheim, 31.12.2024

Contents

List of Figures

List of Tables

1 Introduction

1.1 Motivation & Research Questions

For any continuos system, the ultimate goal is achieving autonomous control at the control layer [1]. The control layer is usually a certain combination of feedback and model based control. Feedback is typically associated with linear PID (Proportional-Integral-Derivative) controllers that only take current and previous measurements in consideration when changing controller output. Perfect control can be achieved if one has perfect knowledge of the system system behaviour. In practice, perfect knowledge rarely exists, which is often why feedback control is used at a short time scale. However, using models in the control layer can often increase setpoint tracking due to active disturbance rejection. There exist "grey box" control methods such as ADRC [2] for increased potential in disturbance rejection. Nevertheless, PID is still the most prevalent method of control in process industry to this day due to its' robustness and simplicity [3].

Higher order economic optimisation problems (time scale: hours) or predictive methods (time scale: minutes) for regulation are not considered in this thesis. Rather, we are interested in the regulatory layer (time scale: seconds)- the layer which is closest to the system itself. Specifically, we look at control of a simple distillation column and an ethyl benzene plant with two reactors and two columns. A method called "bidirectional control" will be used to demonstrate the a dynamic switching of system throughput manipulators by otherwise non-adaptive PID controllers. This method is quite similar to "Split-Range Control" (SRC), which is explained nicely in [1] and [4].

The control method could ideally be implemented in any continuos operation with and without recycle streams and bypasses. The demonstrations will hopefully lead us closer to solving plant-wide control.

All simulations are run in Aspen Plus® using the pressure-driven option. For the purposes of this thesis, it is believed that a physical model with more accurate thermodynamic models will yield superior results compared to a flow-driven model with ideal thermodynamics in Matlab. A drawback of this decision is the lack of flexibility in the Aspen GUI.

1.1.1 Consistency Rules & Inventory Control

It is a prerequisite for a consistent system that all sub-processes are stationary. For a process to be stationary, we also need all inventories I to have a rate of change equal zero ($dI = 0$) at steady-state. The general differential equation is shown in Equation 1.1. Any transient accumulation of inventory must be self-regulated to "stabilize" such that the mass balances are satisfied.

$$dI = (I_{in} + I_{produced}) - (I_{out} + I_{consumed}) \tag{1.1}$$

Definition 1. ***Consistency***. *A system is consistent if the steady-state mass balance (total, component, phases) are satisfied for any and all parts of the process.*

A system can be consistent without necessarily being self-consistent (also called "local consistency"). This implies that all inventories by themselves are not necessarily are consistent, but that the total plant is. Typically, this occurs in plants where "long loops" are used to achieve consistency. Price et al. [5] suggests the following definition.

Definition 2. ***Self-consistency***. *An inventory control structure is said to be "self-consistent" if it is able to propagate a production rate change throughout the process so that such a change produces changes in the flow rates of all major feed and product streams.*

This propagation of change occurs due to local self-regulation at all inventories. The disturbance "radiates" away from the location of the disturbance or the bottleneck.

Definition 3. *A* ***Bottleneck*** *is an active constraint that limits an increase in system throughput (production rate limit).*

In a chemical plant, maximizing product throughput is often of significant economic interest. This means that the bottleneck throughput affects all major feed and product streams. To address this, we introduce the concept of the "Throughput Manipulator" [4–6]. It is worth noting that bottlenecks are typically saturated inputs (e.g., maximum valve openings) rather than intentionally restricted degrees of freedom (TPM).

Definition 4. *A* ***Throughput Manipulator (TPM)*** *is a degree of freedom, typically a valve, that influences the network flow and operates independently of the control actions of individual units, including their inventory control.*

According to [5], TPMs take two different forms: *explicit* manipulators such as product or feed streams and *implicit* manipulators such as heat input or other variables that affect product throughput. In this thesis, no distinction is made between the two.

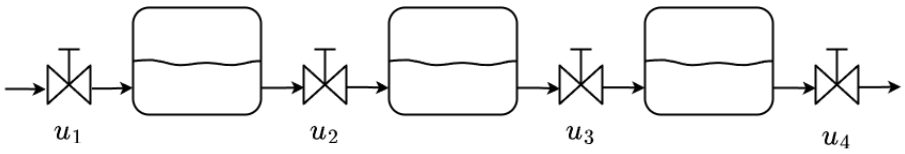

Figure 1.1 – A series of tanks divided by valves (u_i).

Let us start conceptualizing how inventory control works. Consider the simple example shown in Figure 1.1: A series of water tanks with one inlet and outlet each. For this case, we have 3 tanks (N=3) and 4 valves (N+1) to control all inlet and outlet streams. For now we ignore cases with bypass and recycle streams. The objective is to keep the water level in the tanks between a certain interval; not too high and not too low. One valve (input, u) can only regulate one level (controlled variable). The flow rate through a valve is dependent on the pressure before and after the valve, which is shown in Equation 1.2.

$$\dot{m} = f(z) \cdot C_v \cdot \sqrt{\rho \cdot \Delta P} \tag{1.2}$$

Where $f(z)$ is the opening coefficient (between 0 and 1), C_v is the valve constant, ρ is the fluid density and ΔP is the pressure difference across the valve.

Figures 1.2-1.4 illustrate three cases with different control structures for tanks in series. Assume that a pure liquid flow with constant density runs through the valves. Changes in level (inventory) are depicted sequentially using arrows inside the boxes, with adjacent numbers indicating the sequence. Orange arrows represent the radiation response to an increase in throughput, showing how changes in throughput affect tank levels. The controller responding to these changes "radiates" the flow to the next tank as a consequence of local control. In contrast, green arrows represent local inventory control in response to the orange arrows. In other words, radiation (orange) is a consequence of a disturbance or a change in throughput while local inventory control (green) is a controller response to a change in inventory.

Case 1 (Figure 1.2, Self-consistent): The TPM on u_2 decides the throughput. (1) Increasing the flow through u_2 leads to the level in tank 1 to decrease as a consequence. (2) As a response, since the gas volume increases, pressure decrease ($pV = nRT$), and the pressure controller on tank one increases u_1 such that the pressure reaches setpoint. (1) On the other side of the TPM, the level in tank 2 increases which also increases tank 2 pressure. (2) As a consequence, this is relieved by increasing u_3 flow. (3) Then the level in tank 3 increases and u_4 flow increases.

Case 2 (Figure 1.3, Consistent): The TPM at u_2 increases similarly to in case 1. Tank 1 behaves the same as in case 1. (1) When flow to tank 2 increases, the level and pressure increase.

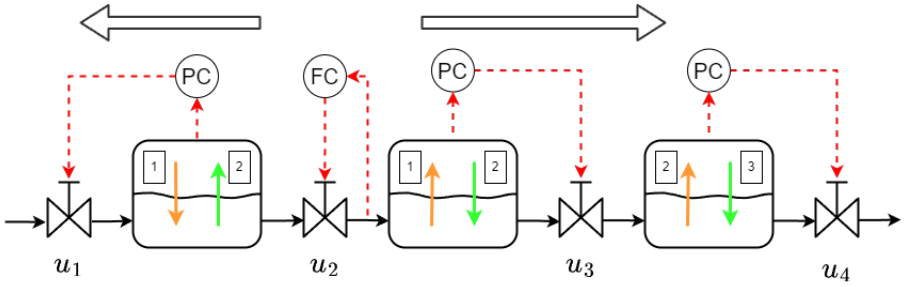

Figure 1.2 – Tank in series with radiation rule applied (self-consistent). Inventory control "radiates" away from the TPM (u_2).

(2) Then, the pressure controller increases u_4 flow. (3) Then, the pressure in tank 3 decreases and valve u_3 opens to equalize the pressure in tank 3 and increases flow from tank 2.

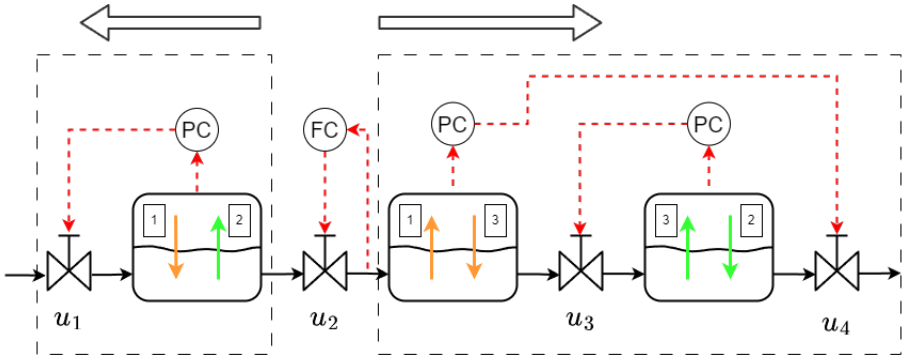

Figure 1.3 – Tank in series with consistent, but not self-consistent, behavior due to the "long loop." The control volumes encapsulated by dashed lines are self-consistent.

Case 3 (Figure 1.4, Inconsistent): The throughput at valve u_3 controlling the flow before tank 2 increases. (1) As a consequence, the level in tank 2 and tank 3 decrease and increase, respectively. (2) Downstream of the TPM, as a response, u_4 is increased to reduce level (OK). (1) Upstream of the TPM, u_2 remains constant since the TPM does not "radiate", which does not increase flow through u_2. This makes the system inconsistent, and the level in tank 2 will decrease until empty.

The system is considered consistent when each tank has one arrow pointing up and one pointing down. If the radiation is "broken off", the system is inconsistent. If the sequence numbers for each tank differ by exactly 1 and the "arrows" have a different colour, the system is deemed self-consistent. Whether these observations hold for all cases of inventory control is unknown.

To summarize the consistency rules for inventory presented by Aske [6]. Rule 1 applies nicely to

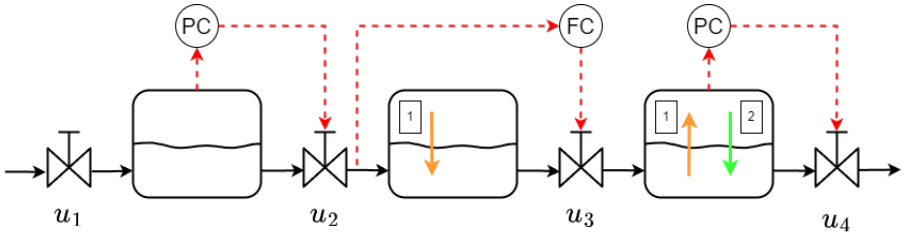

Figure 1.4 – Tank in series with the radiation rule broken.

the 3 examples shown in Figures 1.2-1.4.

1. The total inventory (mass) of any part of the process (unit) must be "self regulated" by its in- or outflows, which implies that at least one flow in or out of any part of the process (unit) must depend on the inventory inside that part of the process (unit).
2. For systems with several components, the inventory of each component of any part of the process must be "self-regulated" by its in- or outflows or by chemical reaction.
3. For systems with several phases, the inventory of each phase of any part of the process must be "self-regulated" by its in- or outflows or by phase transition.

1.1.2 Recycle and Bypass Streams

Some quick remarks have to be made regarding recycle and bypass streams. Recycle streams in an open system (continuos system with feed and product) contain one or more splits that partially feeds back into the system. This increases the degrees of freedom of the system.

1.1.3 Bidirectional Control

We see from Section 1.1 that radiation can work in both directions. Price et al. [5] remarks that, in fact, backwards radiation (opposite direction to flow) can lead to fewer stability problems. This leads naturally to the question: Why not use both simultaneously, and what benefit would this introduce? Intuitively, the TPM would be able to move both backwards and forwards in the plant.

In Figure 1.5, we see how bidirectional control works for two tanks. There are two controllers for each tank, both using the same y value, but different setpoints: SP_H (blue; high) and SP_L (orange; low). A MIN selector for each valve ensures that a bottleneck/TPM can radiate in both directions. As a quick remark, this figure does not feature a TPM, yet we can see that both tanks are self-consistent. The next question comes naturally: how is this implemented in practice?

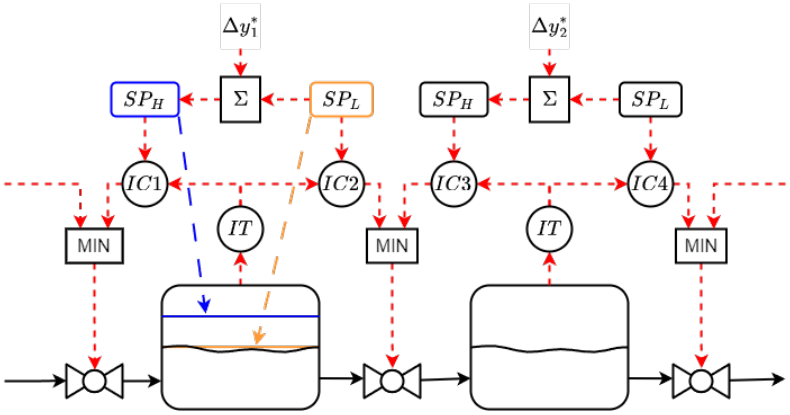

Figure 1.5 – Bidirectional control applied to two tanks with MIN selectors. An inventory transmitter (IT) sends the CV to the inventory controllers. For each tank, there are two controllers. One H-mode (IC1, IC3) with SP_H (blue; control against flow direction) and one L-mode (IC2, IC4) with SP_L (orange; control with flow direction). The minimum controller input is sent to the valve.

1.1.4 (New) Bidirectional Tuning Parameters

Zotica et al. [4] previously introduced and discussed the parameters referred to in this thesis as SP_H and SP_L. They also found promising results using bidirectional control in a series of tanks. The difference between these parameters, denoted as Δy_S^*, is defined in Equation 1.3 as the difference between H-mode and L-mode setpoints. Figure 1.6a) shows how Δy_S^* is defined visually for any H/L controller pair.

$$\Delta y_S^* = SP_H - SP_L \tag{1.3}$$

For level controllers, one has the choice between *tight control* and *averaging control*. The objective of tight control is to keep y close to SP_L. Tight tunings should be adopted for this case with a small Δy_S^*. For averaging control, the objective is to average out flow disturbances by allowing larger variations in level. This is achieved by using smooth tunings and a high Δy_S^*. Also, increasing K_c for a PI controller (see Section 1.2) can increase stability, up until a certain point where instability is inevitable [7, p.220].

By increasing $\Delta y_{S,k}^*$, the time it takes for an inventory controller, IC_k, to reach SP_H increases. This delay can be described approximated using Equation 1.4.

$$\tau_y = \Delta y_S^* \frac{A_{tank}}{\Delta F_k} \tag{1.4}$$

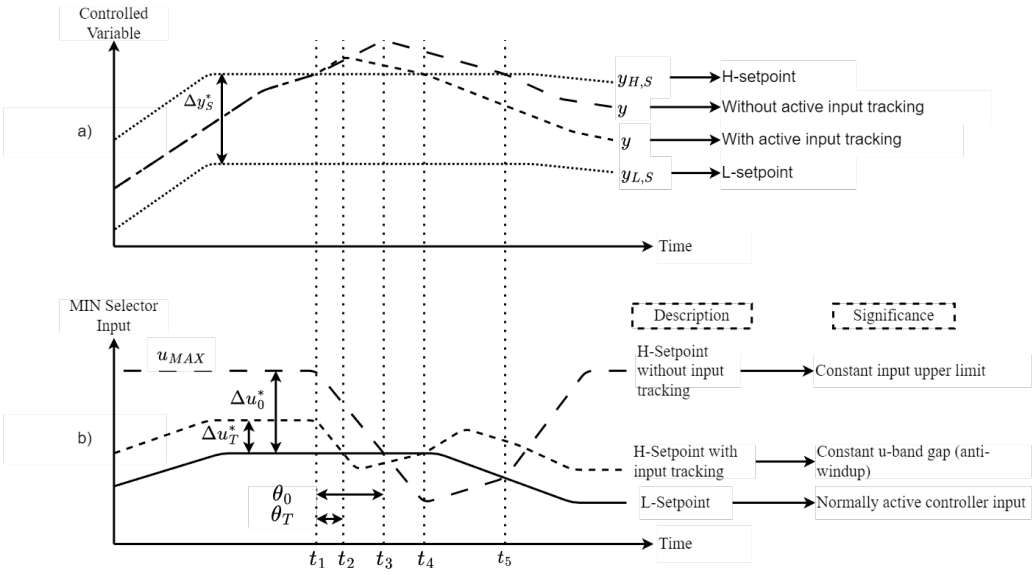

Figure 1.6 – Two cases: Scheme depicting the difference between bidirectional control *with* and *without* input/setpoint tracking on H-controller upper bound. Subfigure a) shows the controlled variable with H and L setpoints. Subfigure b) shows the inputs to controller for the two cases (dashed lines). t_1: $y > y_{H,S}$ and both H-controllers start acting (not yet active in MIN selector). t_2: H-controller with input tracking becomes active in MIN selector, and y starts decreasing after an active delay of θ_T. t_3: H-controller without input tracking becomes active in MIN selector, and y starts decreasing after an active delay of θ_0. t_4: $y < y_{H,S}$ and the H-controller with input tracking becomes inactive. t_5: $y < y_{H,S}$ and the H-controller without input tracking becomes inactive.

Where τ_y is the time it takes from Δy_S^* starts to change (trigger) to the moment Δu_T^* starts to change, A_{tank} is the cross sectional area of the tank and ΔF_k is the accumulated volume flow rate in the tank.

We now introduce the concept of the "input dead band," denoted as Δu^*. As shown in Figure 1.6, Δu^* can be defined either as a constant value (Δu_0^*) or as a tracking value (Δu_T^*). It represents the difference between the current controller output (or manipulated variable input) and the maximum output of the H-controller when the L-controller is active. To ensure proper functionality, anti-windup mechanisms should be implemented. Recommended anti-windup schemes can be found in [1].

$$\Delta u^* = u_{H,\text{inactive}} - u_{\text{MIN,active}} \tag{1.5}$$

A similar remark about the "input dead band" is that increasing Δu^* increases the active delay from when $u_{H,inactive}$ is triggered until u_H becomes active. This delay is denoted as θ_0 and θ_T for

Δu_0^* and Δu_T^*, respectively. This is shown in Figure 1.6b). Both delays are decided by controller tunings and $\Delta u_{inactive}^*$.

1.1.5 The Objective Function

From an economic perspective, maximizing the average throughput, $\bar{F}$, as shown in Equation 1.6a, is a key objective. When bidirectional control is employed, reducing the throughput becomes straightforward: a setpoint is placed on either the product or feed stream, and the TPM radiates throughout the system, provided it is consistent. One of the goal of a bidirectional control system is to dynamically solve Equation 1.6a, since it theoretically should identify TPMs on a global scale.

$$J = \max_u \bar{F} \tag{1.6a}$$

$$\bar{F} = \frac{1}{T}\int_0^T F_k(t)\,dt, \quad k \in [0,\ldots,N] \tag{1.6b}$$

$$\text{s.t.} \quad SP_{L,k}(t) \leq y_k(t) \leq SP_{H,k}(t) \quad k \in [0,\ldots,N] \tag{1.6c}$$

$$u_{\text{active},k}(t) \leq u_{H,k}(t) \leq u_{H,\text{inactive},k}(t) \quad k \in [0,\ldots,N] \tag{1.6d}$$

We then get our first study question.

Study Question 1. ***Economics****: Given a consistent system, what is the ideal choice of bidirectional tuning parameters to maximize and/or average out throughput?*

1.1.6 Bidirectional Control for Larger Plants

The production of ethyl benzene is easily done through a simple reaction between ethyl and benzene shown in reaction 1.7. We may however end up with unreacted product or with di-ethyl benzene shown in Equation 1.8. According to findings by [8], the selectivity of EB increases with the recycle rate of benzene from column 1 or by increasing the reactor size. Also, reducing residence time reduces selectivity of EB.

$$E + B \rightleftharpoons EB \tag{1.7}$$

$$EB + E \rightleftharpoons DEB \tag{1.8}$$

$$DEB + B \rightleftharpoons 2 \cdot EB \tag{1.9}$$

The production of ethylbenzene was the primary example of this task, since there are four processes in a series: two reactors and two distillation columns. Originally, this idea was proposed by Luyben in his 2011 article [8]. Jagtap, Pathak, Kaistha & Gupta iterated on this process in their 2012 article "Economic Plantwide Control of the Ethyl Benzene Process" [9], introducing a highly robust bidirectional control scheme, perhaps as an emergent property of their approach. This work will also build upon and formalize the contributions initiated by Jagtap et al. The control structure by the former authors can be found in Appendix **??**.

> **Study Question 2.** ***Consistency:*** *How can control loops be arranged such that any disturbance or bottleneck in the system radiates away consistently?*

1.2 Controller Tuning

Tuning of controllers greatly affect the system dynamics. Therefore, the following method of tuning is used (prioritized order).

1. The *Skogestad Internal Model Control* (SIMC) rules will be the primary tuning method. These rules, shown in Equations 1.10a and 1.10b, are used to tune all controllers with proportional-integral (PI) action. When multiple controllers are present, sequential tuning via pole-placement (τ_c) will be applied. Responses with integrating action (very high τ) will be tuned using P controllers.
2. The second method will be to use the Ziegler-Nichols "ultimate" gain K_u and period P_u PI-tuning rules [10]. K_c and τ_I are shown in Equations 1.11a and 1.11b, respectively.
3. If all else fails, controllers are tuned based on a combination of engineering intuition and trial-and-error, a common practice in industry.

$$K_c = \frac{\tau}{k}\frac{1}{(\tau_c + \theta)}\ k' = \frac{\tau}{k} \tag{1.10a}$$

$$\tau_I = \min\left(\tau, 4(\tau_c + \theta)\right) \tag{1.10b}$$

Where K_c is the ideal controller gain, τ_I is the integral action constant, τ is the first-order time constant, k is the steady-state gain, τ_c is the tuning parameter and θ is the delay. When transfer functions of higher order than 1 are obtained, the half-rule

$$K_c = 0.45K_u \tag{1.11a}$$

$$\tau_I = P_u/1.2 \tag{1.11b}$$

1.3 Control Elements

1.3.1 The PID controller

The Proportional-Integral-Derivative (PID) controller is one of the simplest forms of feedback control. A measurement error $e_i = y_{S,i} - y_{m,i}$ to track setpoint using a proportional (P), integral (I) and derivative (D) action. The tuning parameters shown in Equation 1.12 (K_c, τ_I and τ_D) are static in a classical PID controller well equipped for linear systems, but less so for non-linear control.

$$u(t) = K_c\left[e(t) + \frac{1}{\tau_I}\int_0^t e(t)\,dt + \tau_D\frac{de(t)}{dt}\right] \tag{1.12}$$

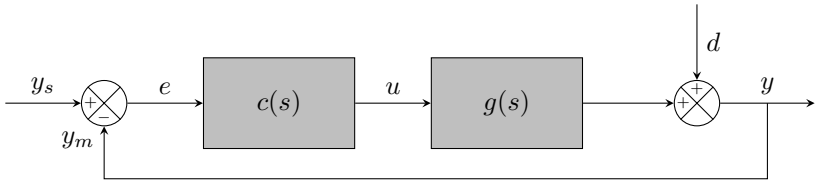

1.3.2 Cascade Control

Nested controllers have the benefit of tracking the setpoint of several MVs using several CVs with different time-scales. According to Skogestad [1], typical values for the time scale separation lies in the range of 4-10. Decreasing the TSS below 3 may introduce coupling between c_1 and c_2, and time scales above 10 is deemed unnecessarily slow.

$$TSS = \frac{\tau_{c1}}{\tau_{c2}} \tag{1.13}$$

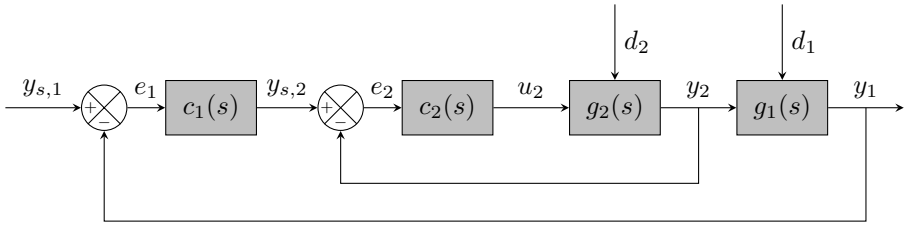

Figure 1.7 – Cascade control block diagram. The "slow" c_2 controller sends a setpoint to the "fast" c_1 controller.

1.3.3 Feed-Forward and Ratio Control

Feed-Forward (FF) offers a simple, yet effective disturbance rejection for processes with large time constants or delays. Disturbances have to be measured directly, and require models to calculate the total controller output, $u_{FB} + uFF$. Contrary to FB, it's only input is a state (not an error), and transforms it before sending an input signal. [7, p.279] There are numerous ways of deciding the FF model, but all of them involve a certain knowledge of system dynamics. A non-linear model will often work for larger ranges for process variables, but may be prone to non-linearities. In Figure 1.8, $g_d(s)$ is usually a linear transfer function (model estimate) to model the disturbance effect on the measured output y_m.

Given an input transfer function g and a disturbance transfer function g_d, the ideal (linear) feed-forward controller. Assume that a measure response can be described using Equation 1.14a. If no feed-forward is implemented, the measured output would simply be $y_m = ecg + dg_d$. To reject most, if not all effects by d on y, c_{FF} should act such that $d(y_m) = s \cdot y_m = 0$. Assuming total disturbance rejection, $e = 0$, which simplifies our expression to Equation 1.14d. Integrating $(1/s)$ and rearranging to Equation 1.14e yields the ("additive") feed-forward controller c_{FF}.

$$y_m = ecg + dc_{FF}g + dg_d \tag{1.14a}$$
$$0 = s \cdot y_m \tag{1.14b}$$
$$0 = ecg \tag{1.14c}$$
$$s \cdot [dc_{FF}g + dg_d] = 0 \tag{1.14d}$$
$$c_{FF} = \frac{-dg_d}{dg} + C_1 = \frac{-g_d}{g} + C_1 \tag{1.14e}$$

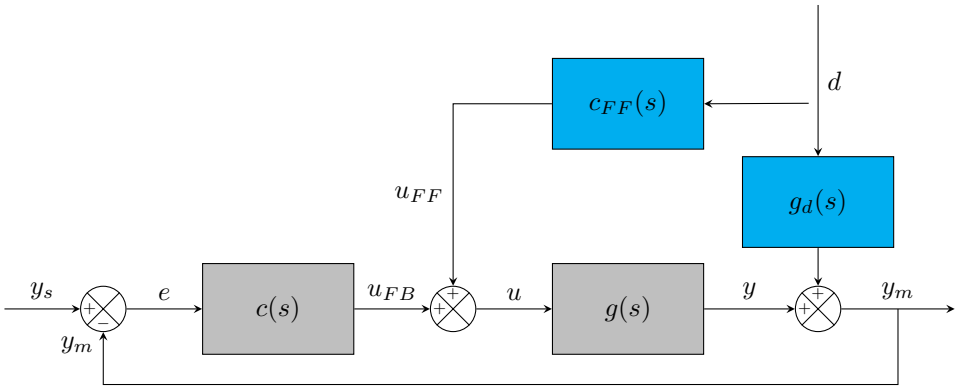

Figure 1.8 – General (additive) feed-forward block diagram. A measured disturbance (d) is transformed using a model (c_{FF}) for additional disturbance rejection.

In a previous study, Luyben [11, 12] describes "additive" and "multiplicative" feed-forward models which share similarities to "additive". Results show that multiplicative feed-forward have slightly better performance.

Ratio Control is a special type of feed-forward that keeps a ratio, usually between two streams, constant. In Section

1.4 Distillation Theory

Distillation is a method of separating components with different volatility. [13, p.29]. In binary distillation, the *relative volatility*, α, is a helpful factor determining how easy it is to separate the two components. In Equation 1.15, "L" and "H" denote light and heavy component while y and x are vapour and liquid molar fraction, respectively [13].

$$\alpha_{LH} \equiv \frac{y_L/y_H}{x_L/x_H} \tag{1.15}$$

Non-ideality in VLE (Vapour-Liquid Equilibrium) will likely exist. α if often assumed constant, but it is rarely the case. An example of this is shown in section 2.1. For a stationary process, the column feed flow (F) must be equal to the sum of distillate (D) and bottoms (B) flow as shown in Equation 1.16a.

$$F = D + B \tag{1.16a}$$

$$\begin{aligned} Fz &= Dx_D + Bx_B \\ &= (F - B)x_D + Bx_B \\ &= Dx_D + (F - D)x_B \end{aligned} \tag{1.16b}$$

Rearranging and solving for D and B (distillate and bottoms rate), respectively in Equations 1.17a and 1.17b, we see that both are functions of F, z, x_B and x_D.

$$D = F\frac{z - x_B}{x_D - x_B} \tag{1.17a}$$

$$B = F\frac{z - x_D}{x_B - x_D} \tag{1.17b}$$

We observe that D and B are functions of F and system purities. Assuming z (disturbance), x_D (setpoint) and x_B (setpoint) are constant, we know that the fractions D/F and B/F must remain constant such that $d(X/F) = 0 \quad \forall X \in \{D, B\}, \ \forall F$. Let us proceed by investigating the distillate only, since balances on D and B are equivalent. We know that D and x_D is constant, V must also be constant. If a disturbance on feed rate is imposed, it follows naturally that the ratio V/F should remain constant for D/F and x_D to remain constant.

1.4.1 Column Composition Control

According to Mejdell and Skogestad [14], logarithmic transforms of purities normalised both dynamic responses and composition profiles. Equation 1.18 can be used to conveniently transform the desired product purity into a linear scale without changing the controller action (reverse/direct).

$$X_i = -log_{10}(1 - x_i) \tag{1.18}$$

Where X_i is the transformed purity at tray i and x_i is the absolute product purity fraction.

1.5 Notation

In this section, notations for controllers and other terms are described in graphical detail for improved readability.

Table 1 describes the letters used to describe controllers. Though in this report, "Transmitter"

(Function) is never used due to redundancy. Controllers without bidirectional override (H) are set as L-mode by default. If controllers are referred to with only two letters (e.g.. "TC"),

Table 1 – Controller Notation. Column #1 denotes what variable type is controlled/transmitted. Column #2 denotes whether the signal is controlled (C) or transmitted (T). Column #3 describes the bidirectional controller mode (normal: Low *or* override: High). Lastly, column #4 describes the specific variable to control.

	1	**2**	**3**	**4**
Description	**Variable type to control** *Intensive variables* T: Temperature C: Composition P: Pressure R: Ratio *Extensive variables* F: Flowrate L: Level	**Function** T: Transmitter C: Controller	**Mode** L: "Low" (Normal) H: "High" (Override)	**Control volume/location** Any stream or control volume descriptor
Example 1 $CT_{H,B}$	C Composition	T Transmitter	H High	B Column bottoms stream (stage 40)
Example 2 $TC_{L,S36}$	T Temperature	C Controller	L Low	S36 Column stage 36

For bidirectional control specifically, there are two signals: L ("Low") and ("High"). In reality, H and L are separate controllers (LC1 and LC2) with different setpoints (SP_H and SP_L) as shown in Figure 1.9a. For simplicity in this paper, the notation in Figure 1.9b is used to describe control structures.

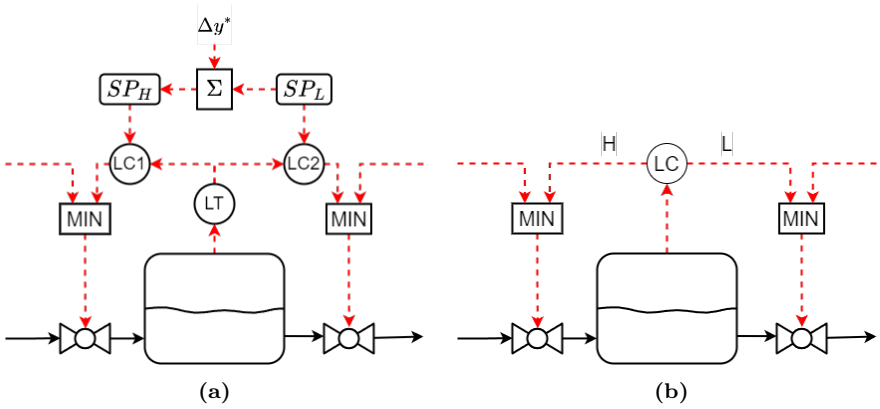

Figure 1.9 – Bidirectional inventory control of a single unit. (a) "Correct" flowsheet with two separate inventory controllers (LC1 and LC2) with different setpoints (SP_H and SP_L). (b) Simplified representation (used in this paper) where one block (LC) represents two controllers and where the setpoints (SP_H and SP_L) are shown indirectly as just H and L (inputs).

2 Dynamic Control of a Distillation Column

All simulations in this section are performed using Aspen Plus® dynamics with a 36 second time interval between each iteration (0.01 hours). For composition controllers, all delays are assumed to be 2 minutes $x_m(s) = x(s) \cdot e^{-\theta s}$. For temperature measurements, all controllers have a lag time constant of one minute $T_m(s) = T(s)\frac{1}{\tau s+1}$.

2.1 Distillation Model (Steady-State)

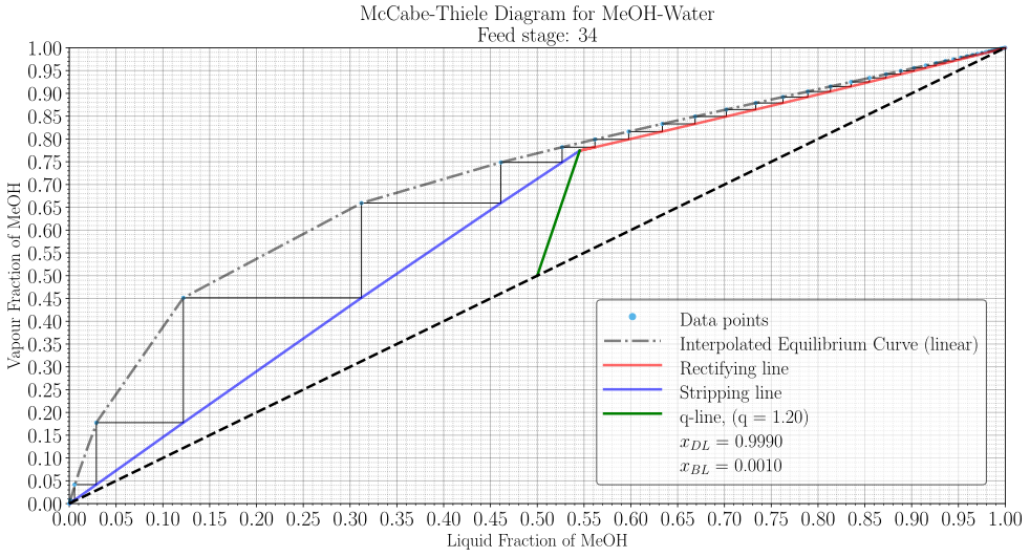

Figure 2.1 – McCabe-Thiele diagram for the water-methanol distillation column.

A relatively simple case is a water-methanol distillation column with 40 theoretical stages is proposed in this section. 50 mole% methanol feed at 20 °C and 2 bar enters the column on stage 34. A total reflux is used as a rectifier with a kettle reboiler at stage 40. The reflux drum and reboiler sump volumes are both set to 3 m^3 with a total height of 3.25 m. Each stage has a diameter of 2 m and spacing of 0.61 m. With a weir height of 0.05 m and 90% active area, the total liquid volume in the column is calculated to $V_{column} = 2 \cdot A_{active}\frac{\pi D^2}{4} \cdot (N_{stages} - 2) \cdot h_{weir} = 10.74m^3$. The NRTL property method is used for state estimation and vapour-liquid equilibrium. The goal of the distillation is to achieve 0.1% impurity in both distillate (light component, methanol) and bottoms product (heavy component, water). As shown in the McCabe-Thiele diagram in figure 2.1, there is a pinching effect above the feed (see rectifying line). This is due to the non-ideal effect between water and methanol at high methanol purities. Consequently, this also means that the stage temperatures near the rectifier change little compared to near the reboiler. This is better illustrated in

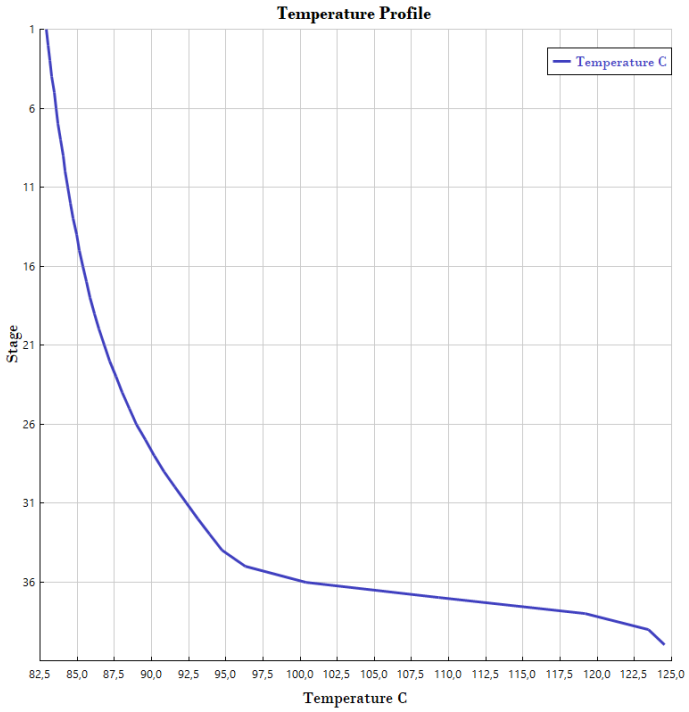

Figure 2.2 – Temperature plot across all stages in the water-methanol column. Stage 1 is the top (reflux) and stage 40 is bottom (reboiler).

Figure 2.2, where we see that the temperatures near the top (low stage number) change little from stage to stage.

All controllers are initialised in when the dynamic simulation runs at steady-state. Values are shown in Table 2.

2.2 Demonstrative Cases and Traditional Approaches

2.2.1 Description

Typical consistent control schemes for distillation columns are shown in in Figure C.1. The first case in Figure 2.3a assumes a constant reflux (L) and reboil (V) flow despite disturbances. The second column in Figure 2.3b shows a case with ratio control (constant ratio) on the reflux L/F and a constant reboil rate. The third column in Figure 2.3c shows a case with ratio control (constant ratio) on the reflux L/F and a temperature control using reboil rate V. The last case in Figure 2.3d shows ratio control (no feedback) on both L/F and V/F. A 10% increase in feed is imposed on all columns as a disturbance.

Table 2 – Summary of controller descriptions for single-column simulations ("BIDIR"). All simulation revisions in Section 2.3 are included. To improve readability, only the controllers that have been modified are shown for consecutive revisions.
(*) Always between MIN and MAX
(**) Changes dynamically for H-mode controllers if input tracking, Δu_T^*, is active (see "BIDIR_2" in section 2.3.3)

Iter.	Controller		CV (y)				MV (u)				
	Type	Mode (H/L)	Description	Initial*	MIN	MAX	Description	Initial*	MIN**	MAX**	Action
1	CC	L	D Purity [-]	0.999	0	1	Stage 36 temperature [°C]	100.36	0	169.88	Direct
	TC	L	Stage 36 temperature [°C]	100.36	0	169.88	Reflux rate [kg/hr]	1621.85	0	3243.7	Direct
	CC	L	B Purity [-]	0.999	0	1	V/F ratio $[\frac{kmol/hr}{kmol/hr}]$	1.1034	0	2.2069	Reverse
	CC	H	B Purity [-]	0.99	0	1	Feed Rate [kmol/hr]	150	40	150	Direct
	LC	L	D Level [m]	1.9	0	3.25	Distillate Valve [%]	24.5	0	100	Direct
	LC	L	B Level [m]	1.9	0	3.25	Bottoms Valve [%]	12.55	0	100	Direct
	LC	H	D Level [m]	2.1	0	3.25	Feed Rate [kmol/hr]	150	40	150	Reverse
	LC	H	B Level [m]	2.1	0	3.25	Feed Rate [kmol/hr]	150	40	150	Reverse
	PC	L	Stage 1 pressure [bar]	2	0	4	Qcond [Gcal/hr]	-0.818	-1.636	0	Reverse
	PC	H	Stage 1 pressure [bar]	2.05	0	4	Feed Rate [kmol/hr]	150	40	150	Reverse
2	CC	L	D Purity [-] ($\log_{10}$ transform)	3	0	6	Stage 36 temperature [°C]	100.36	0	169.88	Direct
	CC	L	B Purity [-] ($\log_{10}$ transform)	3	0	6	V/F ratio $[\frac{kmol/hr}{kmol/hr}]$	1.0427	0	2.2069	Reverse
	CC	H	B Purity [-] ($\log_{10}$ transform)	2.3	0	6	Feed Rate [kmol/hr]	150	40	150	Direct

As a quick remark, the specific values in Table 2 are not represented in these examples. There are also no H-mode controllers present. The column model, flows and setpoints are still the same.

2.2.2 Results and Discussion

Figures 2.4a-2.4d show the responses for flows, logarithmically transformed purities, flow ratios (V/F and L/F), and temperatures on stage 38.

Increasing the feed while keeping V unchanged, as shown in Figures 2.4a and 2.4b, causes the bottoms purity to drop below 90% after 6 hours in B1 and after 3 hours in B2. This difference is due to the ratio control on L/F, which increases L. Additionally, the distillate purity exceeds 99.99%. Therefore, B2 performs worse than B1 in terms of controlling both bottoms and distillate purities.

Unlike B1 and B2, both B3 and B4 increase L and V proportionally to F. This results in both purities remaining close to their setpoints during the runtime. B4, however, demonstrates better initial disturbance rejection, as both V/F and L/F ratios remain largely unchanged. Despite this, B3 outperforms B4 as it employs feedback control on temperature. Since temperature directly influences both bottoms and distillate purity, feedback control provides a significant advantage. Without setpoint tracking in B4, disturbances in feed temperature or composition could lead to

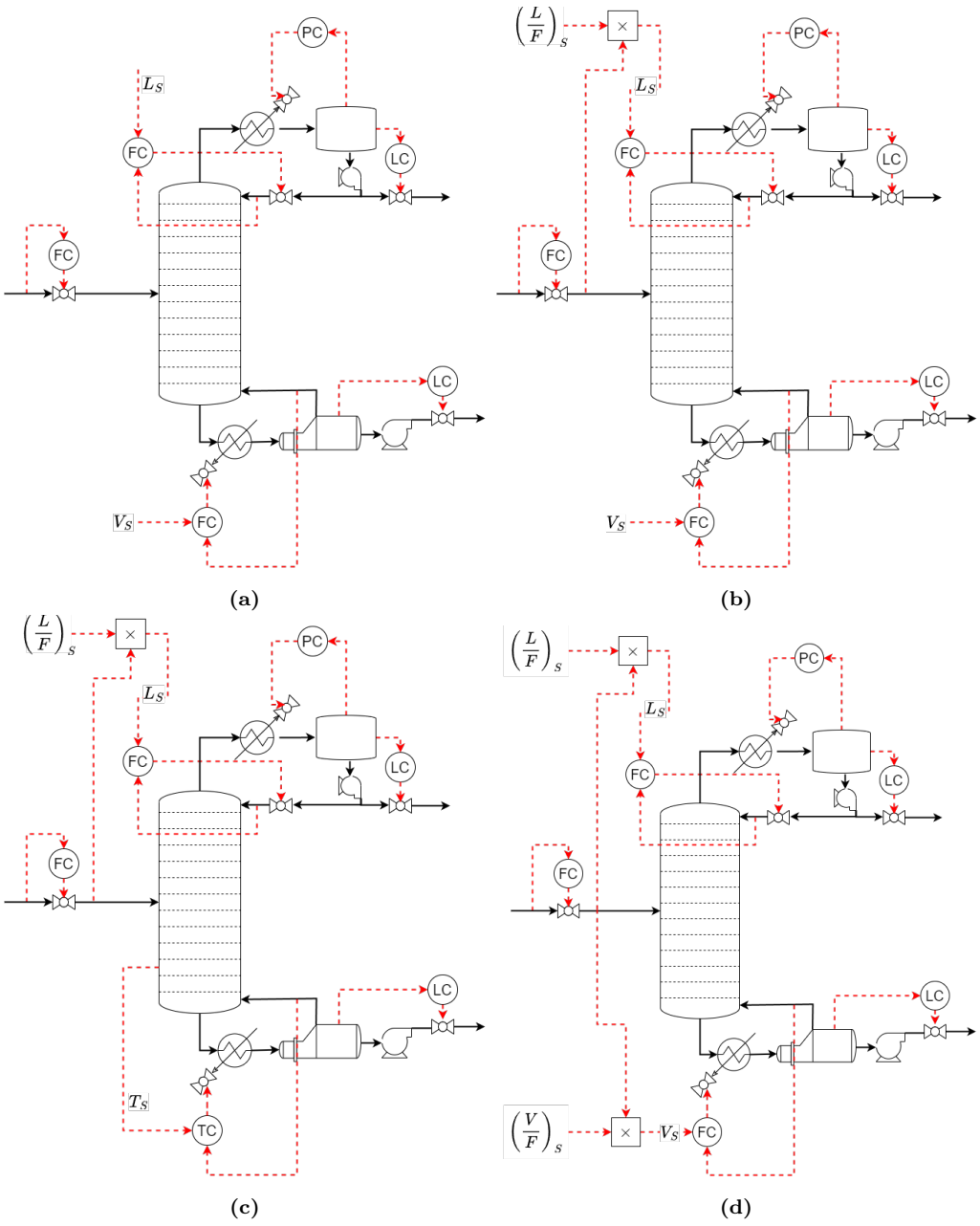

Figure 2.3 – Four "simple" distillation column control schemes.
(a) B1: L and V constant.
(b) B2: L/F and V constant.
(c) B3: L/F constant and temperature control on stage 38.
(d) B4: L/F and V/F constant.

suboptimal results.

The most important finding from this study is the effectiveness of maintaining constant L/F and V/F ratios as part of a feed-forward ratio control design. In theory, it should be equally viable to implement ratio control on L/F with temperature control (TC) on V, and vice versa.

2.3 Bidirectional Logic Approach

Here, we introduce practical cases of bidirectional control. Beginning at the "simplest" example, namely the distillation column in section 2.1, we use our understanding of the column dynamics to create a reasonable control scheme. We iterate to achieve a robust using all degrees of freedom. Using the results from this study, we then introduce the column control logic to a larger system, namely the ethyl benzene plant in section 3.

2.3.1 Iteration 1: BIDIR_1

The main purpose of this example is to illustrate how bidirectional control (aka. override control) can work specifically for a distillation column with sub-cooled feed ($q_F > 1$) as well as showcasing some specific challenges the design may face.

The preliminary though process behind the control design scheme shown in Figure 2.5 is logical. Firstly, we are interested in maximizing throughput while keeping both distillate and bottoms impurities to 0.1 mole%.

Starting at the distillate composition, we use a typical cascaded design with a slow composition controller ($CC_{L,D}$) sending a setpoint temperature to the fast temperature controller ($TC_{L,S36}$) at the reflux valve. In typical columns, the valve would usually be placed close to the top of the column due to the "close pairing" rule of thumb. However, due to the "pinching" effect shown in Figures 2.1 and 2.2, the open-loop gain from reflux to temperature on stages 1-20 is low. Therefore, the temperature controller is placed at stage 36; 2 stages below the feed inlet and 3 stages above the reboiler. For the bottoms composition controller ($CC_{L,B}$), it adjusts the reboiler duty (Q_{Reb}) using both the composition error and feed rate. Under ideal conditions with no disturbance on either feed composition or temperature, the reboiler duty is directly proportional to the boil-up rate (V). And since mass balances for the system must comply given a constant product composition, we can assume that the ratios $\frac{V}{F}$ and $\frac{L}{F}$ should remain constant. The bottoms L-mode composition controller therefore adjusts the reboil-to-feed fraction, $\left(\frac{V}{F}\right)_S$, which is multiplied by the current feed rate F. This yields the reboil rate set-point (and consequently required reboiler duty), $V_S \propto Q_{Reb}$.

When the bottoms composition controller is lost (i.e. V reaches V_{MAX}), the composition controller instead switches to H-mode to reduce feed rate setpoint through the MIN selector at CV1. Then,

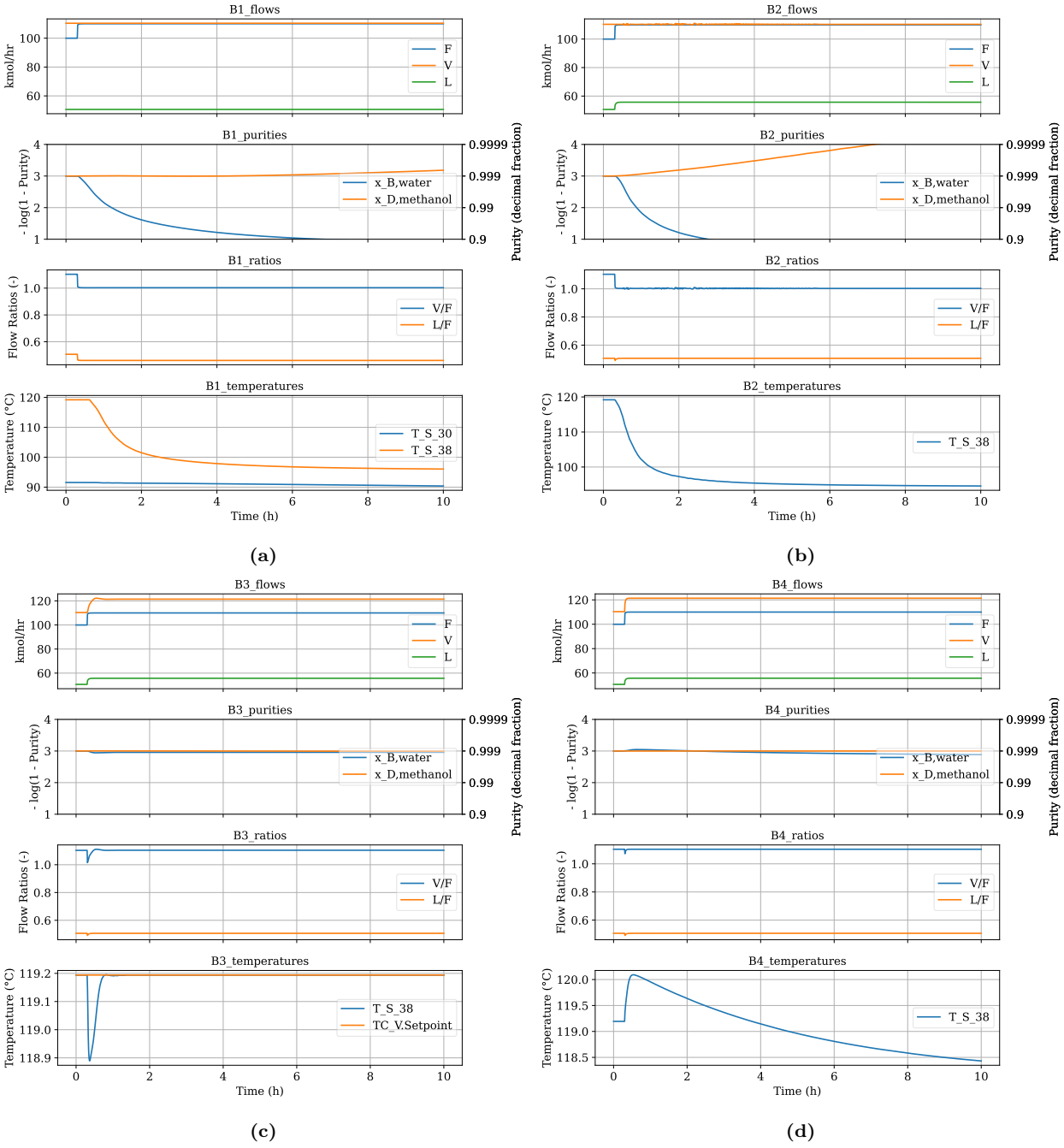

Figure 2.4 – Feed disturbance (+10%) simulation results from the schemes in Figure 2.4.
(a) B1: L and V constant.
(b) B2: L/F and V constant.
(c) B3: L/F constant and temperature control on stage 38.
(d) B4: L/F and V/F constant.

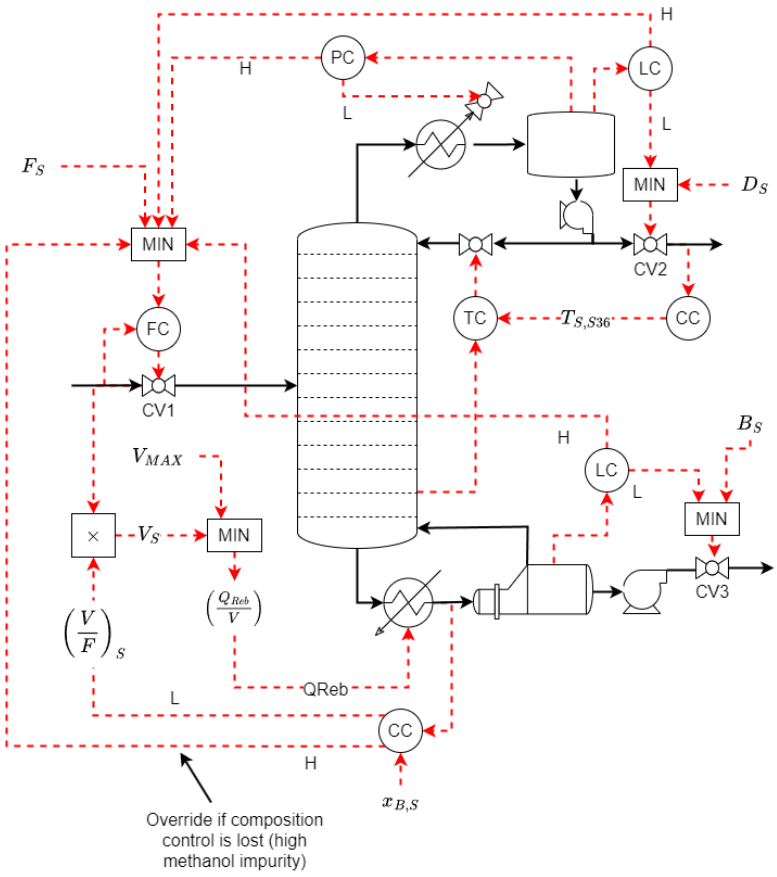

Figure 2.5 – Bidirectional control for a simple distillation column.

the steady-state bottoms water composition becomes 99.0% (log 2) instead of 99.9% (log 3). This works since water is not the important product.

The column pressure is also regulated nominally using a condenser heat exchanger ($PC_{L,Cond}$). When this heat rate reaches max ($Q_{Cond} = Q_{Cond,MAX}$) the column pressure will increase globally. Intuitively, one would choose to then reduce the reboiler duty (V) directly through manipulating Q_{Reb}. However, reducing the feedrate also reduces the reboiler duty since to F directly affects V through the feed-forward ratio control (V/F_S). Placing the override signal from the pressure regulator directly on the reboiler duty will instead cause the bottoms composition to reduce so that $CC_{H,B}$ or bottoms level override $LC_{H,B}$) to reduce F. This extra step should also work, naturally increases the effective delay until steady-state.

The simulations in Figure 2.6 show clearly the effectiveness of the advanced bidirectional (override)

control strategy, and that it handles changes in the TPM location, where different MVs may saturate (see details in Table 4).

Table 3 – Tuning parameters for the distillation column in Figure 2.5. The controllers were tuned sequentially in the order given in the table. From the desired τ_C, we obtain K_C and τ_I from the SIMC rules and open-loop experiments performed in Aspen Plus. The controllers marked (*) were tuned manually based on qualitative process dynamics.

Controller	τ_C [s]	K_C	τ_I [s]	**Setpoint**
$LC_{L,D}$	*	-50	7200	1.9 m
$LC_{L,B}$	*	-50	7200	1.9 m
$PC_{L,S1}$	100	3	28	2.0 bar
TC_{S36}	60	5.3	2336	set by CC
CC_D	600	-528	3600	1.e-3
$LC_{H,D}$	*	10	7200	2.0 m
$LC_{H,B}$	*	10	7200	2.0 m
$PC_{H,S1}$	*	1	3600	2.05 bar
$CC_{L,B}$	*	7.95	7500	1.e-3
$CC_{H,B}$	*	1	600	1.e-2

Table 4 – Summary of constraint limit changes that result in activating H-overrides that result in moving the TPM in Figure 2.12.

Time (h)	**Throughput manipulator (TPM)**	**Initial value**	**New Limit**
0.5	F_s [kmol/h]	100	140 (+40%)
10	CV3 (bottoms valve)	31.98%	22.39% (-30%)
20	CV2 (distillate valve)	44.90%	31.45% (-30%)
30	QCond [Gcal/hr]	-0.963	-0.867 (-10%)
40	QReb [Gcal/hr]	1.107	0.997 (-10%)

At t=0.5 h, the feed rate is increased by 50%, and this is handled nicely without any overrides being activated (as no constraints are encountered). Thus, the location of the throughput manipulator (TPM) remains at the feed. The location of the TPM is seen from the subplot "Select Minimum Feed Flow" which shows the five inputs to the feed MIN-selector. Initially, the blue line FC_F is the minimum, which means that the TPM is at the feed. Notice in "Select Minimum Feed Flow" that the green line ($LC_{H,B}$) almost becomes active, but returns to nominal quite fast.

At t=10 h, a constraint on the bottom flow (CV3) is introduced (so that this becomes the TPM). Initially, we lose control of bottom (sump) level, but as the bottom level approaches the H-setpoint (2.1 m), the H-override bottom level controller ($LC_{H,B}$) is activated and reduces the desired feedrate, which at about t=13 h becomes the actual feedrate. This happens at the time where the green line

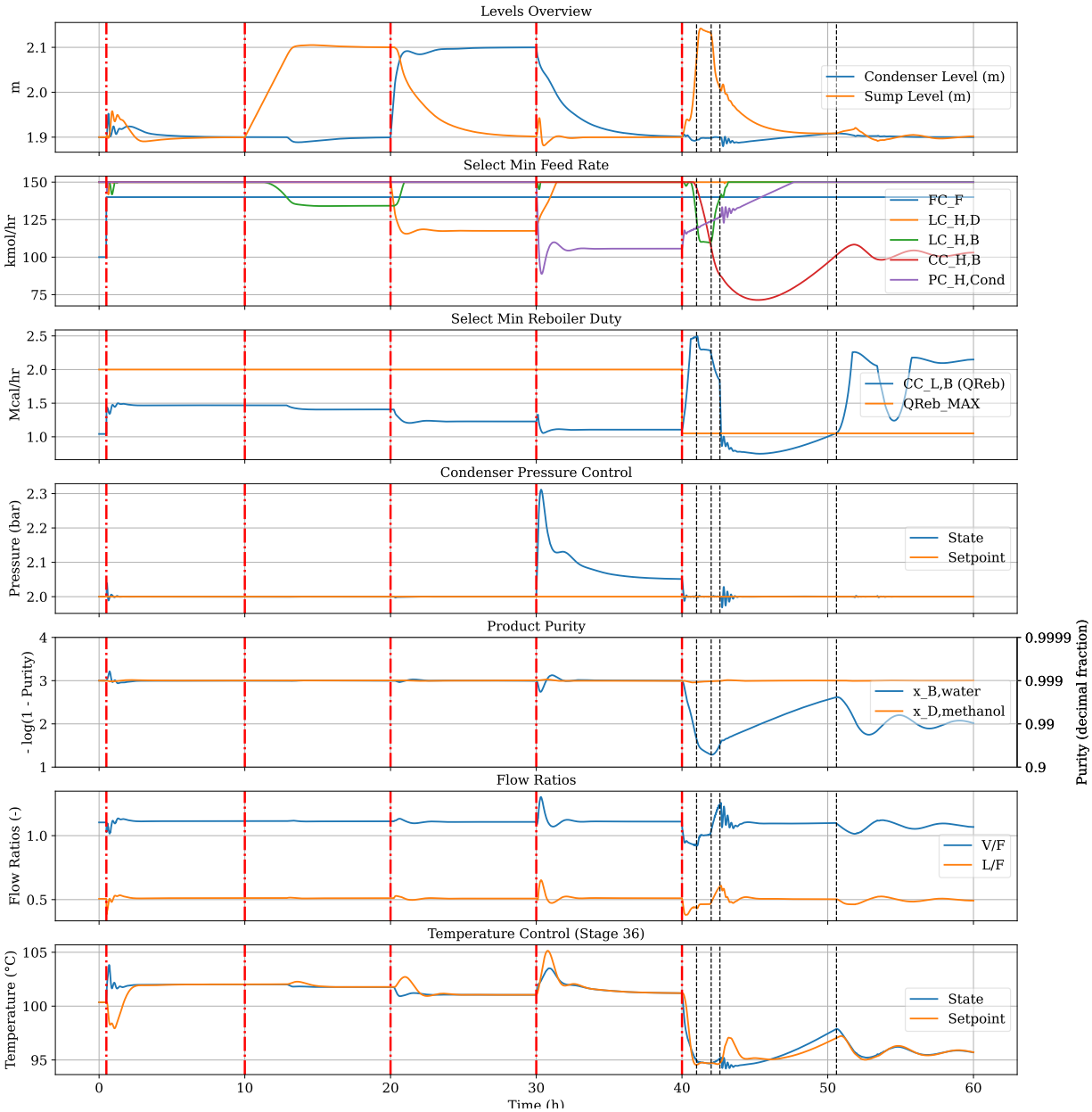

Figure 2.6 – BIDIR_1: 60 hour simulation to illustrate dynamic TPM transfer/radiation. Vertical red lines indicate events where MVs are saturated manually. These events are described in Table 4.

is the smallest in the subplot "MIN-selector for feed flow".

Next, at t=20 h, a constraint on the distillate flow (CV2) is introduced, so that we lose control

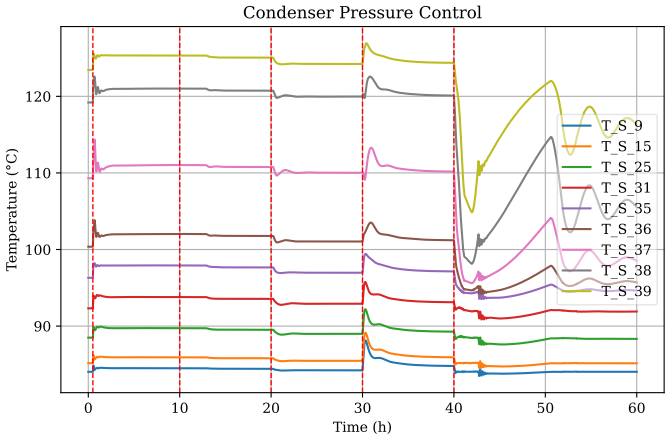

Figure 2.7 – Temperature profiles for "BIDIR_1"

of top (condenser) level. The H-override condenser level controller ($LC_{H,D}$) reduces the desired feedrate, which shortly after becomes the actual feedrate (at the time where the orange line is the smallest in the subplot "MIN-selector for feed flow"). Through the V/F ratio control, this reduces the boilup V and condenser level is stabilized at the H-value (2m).

Next, at t=30 h, a constraint on the cooling duty (Q_{Cond}) is introduced, so that we lose control of pressure. The H-override pressure controller ($PC_{H,D}$) (which is a bit slow) reduces the desired feedrate, which shortly after becomes the actual feedrate (at the time where the purple line is the smallest in the subplot "MIN-selector for feed flow"). Through the V/F ratio control, this reduces the boilup V and pressure is eventually stabilized at the H-value (2.05 bar).

Finally, at t=40 h, a constraint on the heating duty (Q_{Reb}) is introduced, which is equivalent to a max-constraint on boilup V (V_{MAX}), so that we lose control of bottom composition and the feedrate needs to be reduced further. Four events are marked in dashed vertical lines at $[t_1, t_2, t_3, t_4] = [41, 42, 42.6, 50.6]$ hours. Initially at t_1, before the H-mode composition controller ($CC_{H,B}$) activates a reduced feedrate, there is a loss of control of bottoms (sump) level ($LC_{H,B}$ activates), which results in an additional reduction in feedrate (see green line at t_1). While $LC_{H,B}$ Then at t_2, $CC_{H,B}$ becomes active and reduces feedrate. While this occurs, we know that $CC_{L,B}$ is attempting to increase bottoms purity $x_{B,water}$ by increasing V despite being inactive. Consequently, V/F_S saturates Because of this, the "normal" composition controller ($CC_{L,B}$) temporary becomes active and tries to bring the composition back to its "normal" $SP_L = 1 \cdot 10^{-3}$ (log=3) (see "MIN-selector for reboiler duty" subplot).

The result of these interactions between the H-overrides for bottom composition and bottom level is that it takes about 20 hours before the bottom impurity (methanol) is reduced from $SP_L = 1 \cdot 10^{-3}$ and stabilizes at $SP_H = 1 \cdot 10^{-2}$. One is to change the H-setpoint to a value closer to the L-setpoint (e.g., to $SP_H = 2e^{-}2$), a second is to use higher controller gains in the H composition controller ($CC_{H,B}$), and a third is to introduce tracking for anti-windup ($CC_{H,B}$) so that the controller output (red line in "Select minimum feed flow" subplot) does not start so far away (150 kmol/h) from the present value (105 kmol/h). All of these measures reduces the time for the H-override composition controller ($CC_{H,B}$) to activate and reduce the feedrate. A fourth possibility would to increase the sump level H-setpoint (e.g. from $SP_H = 2m$ to $SP_H = 2.5m$) to delay the time before $CC_{H,B}$ is activated. In any case, the simulations in Figures **??** and 2.7 demonstrate the robustness of the proposed control architecture.

2.3.2 Interim Analysis of "BIDIR_1"

There are several available measures to improve the plant performance which are summarised below. Considering how well the column handles a feed increase (FC_F, t=0.5 hr), bottoms valve saturation ($LC_{H,B}$, t=10 hr), distillate valve saturation ($LC_{H,D}$, t=20 hr) and ($PC_{H,Cond}$, t=30 hr) worked in iteration 1, we will only consider the case where reboiler duty is saturated from now on in discussions.

1. Firstly, the composition controllers for D and B both read absolute impurity fractions. Transforming all purity outputs (or rather impurities) using Equation 1.18 should therefore yield a more linear response. This linearity is also evident in the open-loop responses shown in Tables 5 and 6.

2. Secondly, there is the issue of CV setpoint dead-band, Δy_S^*. For the composition controllers, $SP_L = 1e^{-}3 = log[3]$ and $SP_H = 1e^{-}2 = log[2]$ such that $\Delta y_S^* = log[3] - log[2] = log[1] = 0.1$. To get a faster override from $CC_{H,B}$, SP_H can be set to log[2.3] = 0.995 instead. In addition, the bottoms purity will be higher. For the level controllers, we have $SP_L = 1.9m$ and $SP_H = 2.1m$. Increasing SP_H to 2.5 m should increase τ_y. This also reduces back-off for the bottoms product.

3. Thirdly, for level controllers, we can significantly reduce the controller gain to introduce an averaging (buffer) effect on the plant.

4. Next, we can introduce input tracking for anti-windup (Δu^* defined in Equation 1.5) so that the controller output (red line in "Select minimum feed flow" subplot) does not start too far away from the present controller output. For example, the initial inputs for the H-mode controllers ("Select Minimum Feed Flow": 150 kmol/", "Select Minimum Reboiler Duty": 2 Gcal/hr") affects the effective delay for when the "override" controller becomes active. This

is illustrated in Figure 1.6b). Δu_T^* should be used for tracking. In Aspen Plus® V14, there is unfortunately no simple way of achieving this. Manual input tracking should therefore be performed instead.

5. Lastly, the tuning of all H-mode controllers were tuned arbitrarily. Ideally, the the feed-to-variable transfer function ($G_F(s)$) or reboiler-to-variable transfer function ($G_{QReb}(s)$) should be identified in order to obtain ideal tuning ("variable" can be level, composition, temperature etc.). For example, the reboiler-to-x_B_water controller ($CC_{L,B}$) was not ideally tuned, which was likely the main reason slow oscillations were observed.

2.3.2.1 Open-Loop Response for L-mode Composition Controllers

Figure 2.8 and Table 5 present the open-loop results for the bottoms purity composition when the reboiler duty is increased or decreased by 5% (step). The response parameters $k_{\log}$, $\tau_{\log}$, and $\theta_{\log}$ are of the same order of magnitude for the log-scale step response. In contrast, for the decimal-scale step response, both the gain difference, $k_{\text{lin},-5\%}/k_{\text{lin},+5\%} = 87.6$, and the delay difference, $\theta_{\text{lin},-5\%}/\theta_{\text{lin},+5\%} = 34.6$, deviate significantly from unity. A similar analysis was performed for the distillate L-mode composition controller, and results are shown in Table 6.

An important note for both open-loop experiments performed on $CC_{L,D}$ and $CC_{L,B}$ is that the experiment time span greatly affects the loop characteristics from the automatic results obtained directly from Aspen Plus®. Here, the MV step occured at t=1 hours and lasted until t=5 hours. This is likely due to the Aspen Plus® loop analyser being inconsistent, and in some cases giving wrong results. To circumvent this, one may manually read data to obtain the initial slope and delay of the response curve.

Table 5 – $CC_{L,B}$: ±5% open-loop step increase in reboiler duty, and response in purity (linear scale vs. log scale) was measured using Aspen Plus® loop analyser (Automatic).

Reboiler Duty	**+5 %**	**-5 %**	**Method**
k **(linear)** [%/%]	0.0197	1.7252	Automatic
τ **(linear)** [s]	1167.8	4059.5	Automatic
θ **(linear)** [s]	104.8	6734.2	Automatic
k **(log)** [%/%]	8.35	11.05	Automatic
τ **(log)** [s]	5456.8	6960.7	Automatic
θ **(log)** [s]	270.7	272.8	Automatic

Either way, since the time constant is in the time scale of hours, both composition controllers should be slow such that the setpoint to the fast temperature controller and V/F_S.

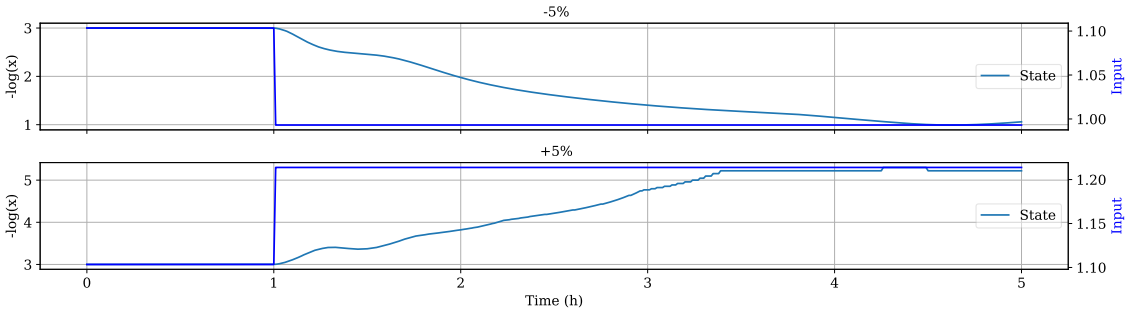

Figure 2.8 – Open-loop experiment from the reboiler (Input: Reboiler Mcal/hr) to the bottoms composition controller in Figure 2.5 (BIDIR_1) (x: absolute composition, State: transformed absolute composition). First-order response parameters are shown in Table 5.

Table 6 – $CC_{L,D}$: ±2% open-loop step increase in stage 36 temperature setpoint (cascade to TC_{S36}), and response in log-scale purity measured using Aspen Plus® loop analyser (Automatic). Step at t=1 hr and end experiment at t=5 hr.

Stage 36 temperature	**+5 %**	**-5 %**	**Comment**
K_u **(log)** [%/%]	-10.55	-9.66	Automatic
τ_u **(log)** [s]	7889.1	9220.35	Automatic

2.3.2.2 Closed-Loop Auto-Relay Tuning (ZN)

Figure 7 shows the closed-loop auto-tune experiment performed on both $CC_{L,B}$ and $CC_{L,D}$. When optaining the ultimate gain K_u and time constant τ_u, we use Equations 1.11a and 1.11b to obtain tuning parameters. Since the composition controllers are supposed to be slow,

Table 7 – $CC_{L,D}$ ±2% closed-loop relay auto-tuning for $CC_{L,B}$ and $CC_{L,D}$ (cascade to TC_{S36}). and response in log-scale purity measured using Aspen Plus® loop analyser (Automatic). Step at t=1 hr and end experiment at t=5 hr.

	$CC_{L,D}$	$CC_{L,B}$	**Comment**
K_u **(log)** [%/%]	6.18	1.23	Automatic
τ_u **(log)** [s]	2016	1764	Automatic
K_c **(Eq. 1.11a)**	2.78/3	0.554/3	Divide gain by 3
τ_I **(Eq. 1.11b)**	1680	1470	

2.3.2.3 Effect of Δy_T^* and Δu_T^*

Figure 2.10 shows how different values for Δy_S^* will affect the effective delay, τ_y. Next experiment in Figure 2.11, we investigate how a change in Δu_T^* changes the effective delay, θ_T, of $CC_{H,B}$. In contrast to the experiment in Figure 2.10, the integral action is increased to $\tau_I = 1hr$ such that we approach SP_H.

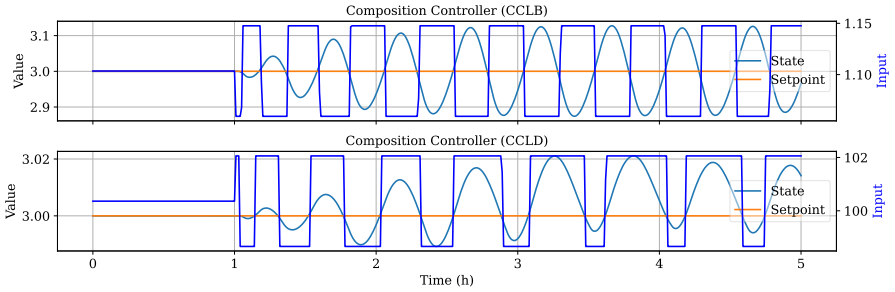

Figure 2.9 – Closed-loop ATV experiment in Aspen for $CC_{L,B}$ (top) and $CC_{L,D}$ (bottom). Value/state/setpoint: $-log(x_{impurity})$, Input: $TC_{S36,S}$ for $CC_{L,D}$ and V/F_S for $CC_{L,B}$.

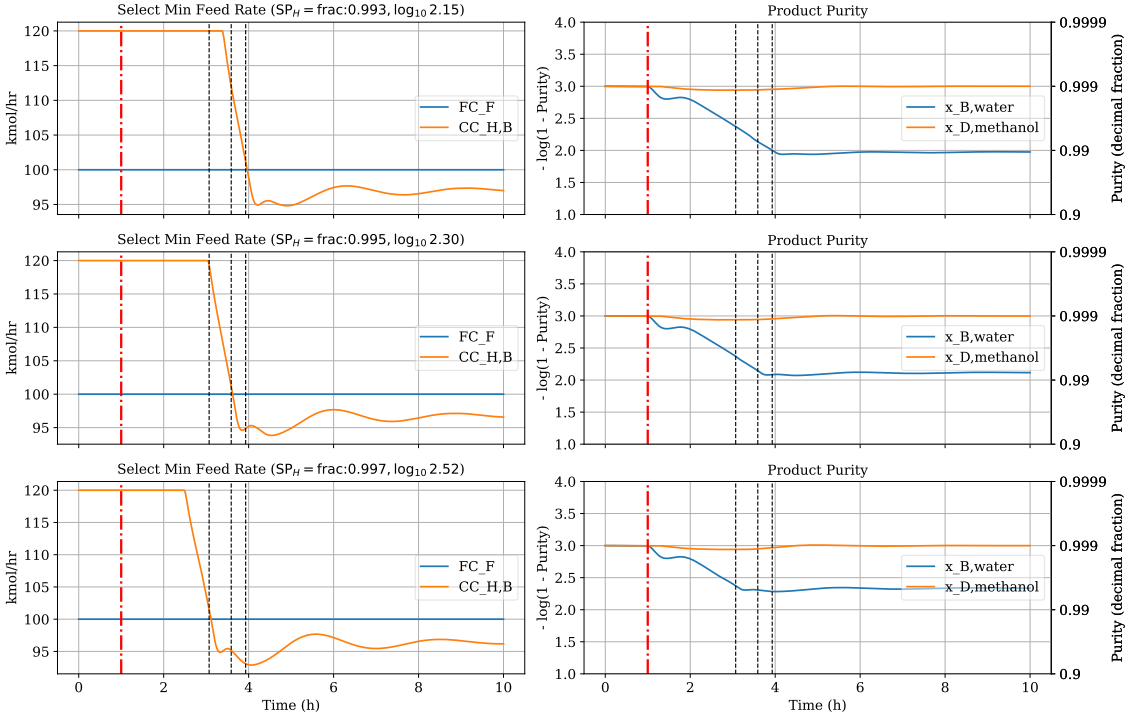

Figure 2.10 – "BIDIR_2" Δy_T^*-test: Override composition control ($CC_{H,B}$) when $V = V_{\text{MAX}}$. Q_{Reb} is decreased by 5% from steady-state to saturation (from 1.04 to 0.999 Gcal/hr) at $t = 1\,\text{hr}$. The tracking input bandwidth (u_T^*) is 20% of the current input for all cases, $\Delta u_T^* = 0.2u_L$. Meanwhile, the setpoint bandwidth (Δy_S^*) is is 0.06 (log 2.15), 0.04 (log 2.30), and 0.02 (log 2.52) for the top, middle, and bottom plots, respectively.

From this, we can confirm that decreasing Δy_S^* decreases τ_y. Likewise, decreasing Δu^* decreases Δu^*. Controller tuning has a great effect on τ_y as well. Assuming that the inactive H-mode

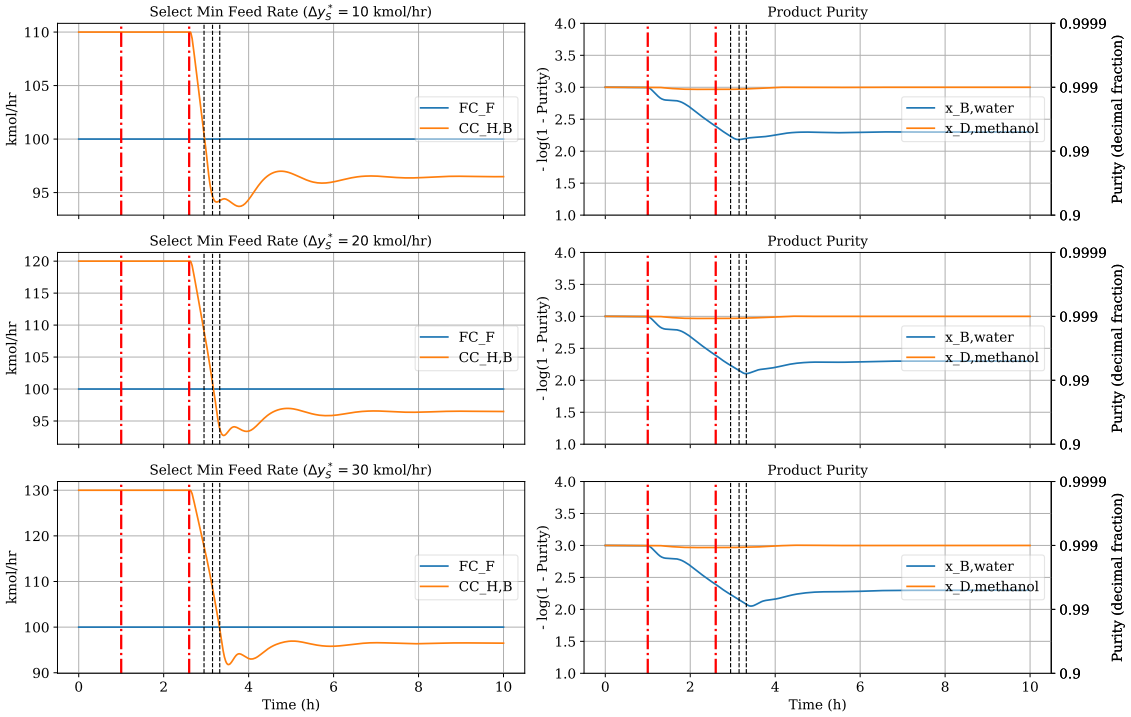

Figure 2.11 – "BIDIR_2" Δu_T^*-test: Override composition control ($CC_{H,B}$) when $V = V_{\text{MAX}}$. Q_{Reb} is decreased by 5% from steady-state to saturation (from 1.04 to 0.999 Gcal/hr) at $t = 1\,\text{hr}$. The tracking input bandwidth (u_T^*) is 10%, 20% and 30% of the current input for all cases. The setpoint bandwidth (Δy_S^*) is 0.04 (log 2.30) for all cases.

$y_{H,inactive}$ is linear, solving equation.

$$\tau_y = \frac{\Delta y_S^*}{s \cdot y_{H,inactive}} = k_y' \frac{1}{s} \tag{2.1a}$$

This equation will not be used, but could be convenient for further use.

2.3.3 Iteration 2: BIDIR_2

Suggestion 1, 2, 3 and 4 in Section 2.3.2 were introduced for this iteration. SP_H for $CC_{H,B}$ is adjusted from log 2 to log 2.3. $K_c = 0.6$ for $CC_{L,B}$ and $CC_{H,B}$, but. SP_H for $LC_{H,B}$ and $LC_{H,B}$ increased to 2.5 m from 2.1 m. Gains for for both level controllers were reduced from -50 to -5. For MIN_F, the input dead band was chosen as $\Delta u_T^* = 10$ kmol/hr. Since implementing a dynamic input tracking (Δu_T^*) in Aspen is non-evident, it was done manually by changing the H-mode

controller limits at the beginning of each event.

Table 8 – Updated tuning parameters for the simulation in Figure 2.12. The rest are idential to

Controller	τ_C [s]	K_C	τ_I [s]	**Setpoint**
$LC_{L,D}$	*	-5	7200	1.9 m
$LC_{L,B}$	*	-5	7200	1.9 m
$CC_{L,D}$	*	3	3600	1.e-3
$CC_{L,B}$	*	0.5	3273.6	1.e-3
$CC_{H,B}$	*	0.6	3600	1.e-2

Table 9 – Summary of events and constraint limit changes. Each row highlights the saturation of a manipulated variable and the corresponding new steady-state or setpoint values.
(*) Both $CC_{H,B}$ and $LC_{H,B}$ have their upper limits set to 112.97 kmol/hr.

Time (h)	**TPM**	**Initial Value**		**New Value**	
		F_S **(kmol/hr)**	**MV**	F_T **(kmol/hr)**	**MV**
0.5	F_s [kmol/hr]	100	–	140 (+40%)	–
10	CV3 (bottoms valve %)	140	31.67	150	19.00 (-40%)
20	CV2 (distillate valve %)	129	37.43	139	29.95 (-20%)
30	Q_{Cond} [Gcal/hr]	114.46	-3.926	124.46	-3.533 (-10%)
40*	Q_{Reb} [Gcal/hr]	102.97	1.077	112.97	1.023 (-5%)

The simulation in Figure 2.12 shares many similarities with "BIDIR_1". Firstly, since the level controller gains were reduced by a factor of 10, we see more averaging level control in "Levels Overview". For a single column with small holdup volumes (3 m^3), this may have little effect on the throughput. The biggest change happens at t=40 when the reboiler duty becomes a bottleneck. Δy_S^* is log 2.3 instead of log 2.0, which means that τ_y becomes smaller. Also, we see that $CC_{H,B}$ and $LC_{H,B}$ (inactive) input follows the active input in "Select Min Feed Rate" (only 10 kmol/hr above). For BIDIR_2, τ_y is 1 hour, and settles quickly without oscillations. Compared to BIDIR_1 where τ_y is approximately 2 hours oscillates after. The oscillations are very likely a cause of the non-linear gain for pure composition.

The improvement of from BIDIR_1 to BIDIR_2 is clear.

3 Ethylbenzene Plant with Bidirectional Control

3.1 Operating Conditions

The simulation conditions are the exact same as "Mode I" in [9]. An adapted version of the flowsheet they used can be found in Appendix A. The tables in Appendix B (Table 11 and 12) show

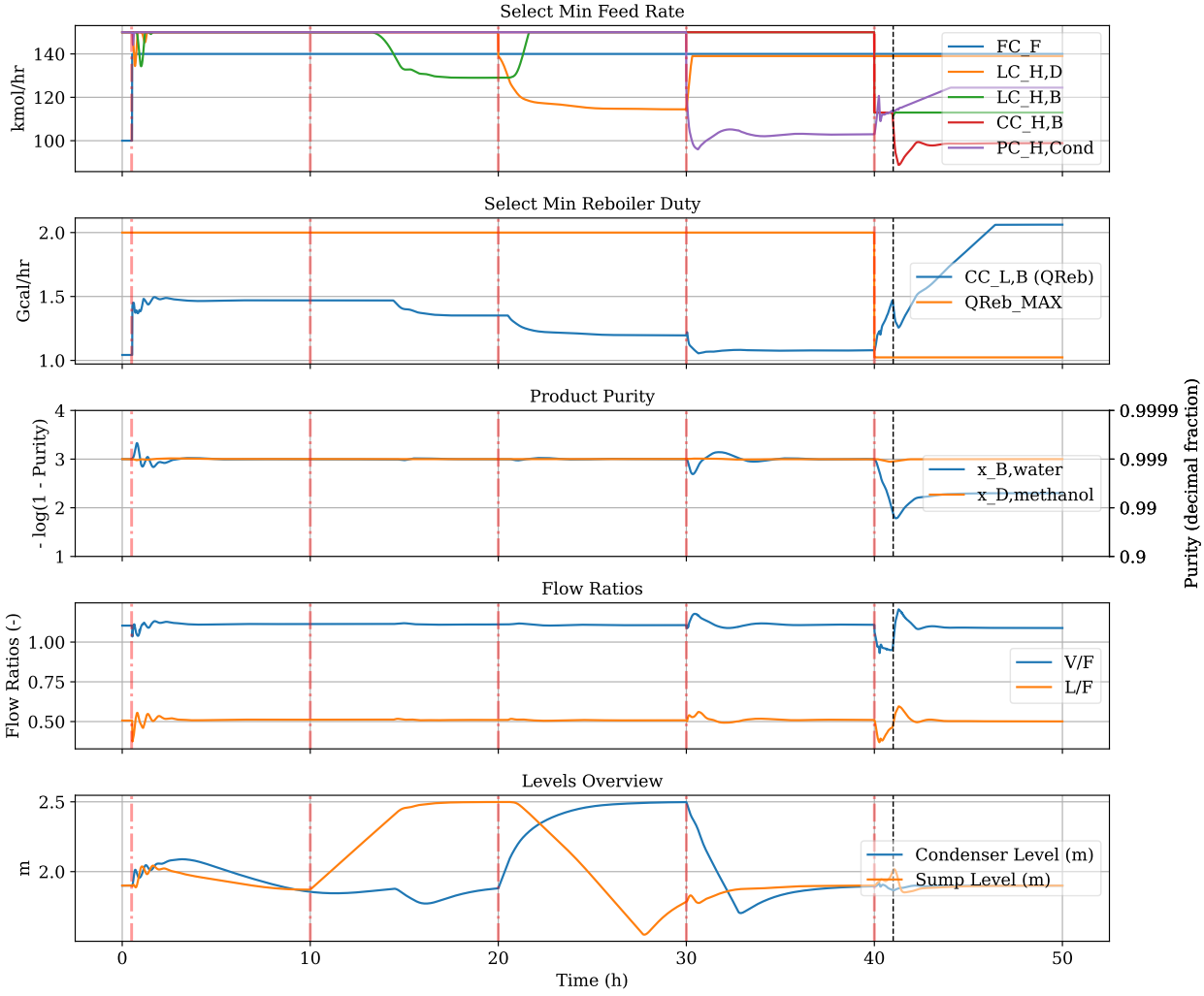

Figure 2.12 – BIDIR_2: 50 hour simulation showcasing sequential introduction of bottlenecks at t=0.5, 10, 20, 30 and 40 hoours. Events are described in Table 9.

the steady-state operating conditions both reactors and columns. Appendix C show the steady-state compositions for the columns. For more detailed information on ideal operating conditions, it is recommended to read the original authors' article.

3.2 Control Structure Design

Appendix D shows the controller tunings used for the entire EB plant in this section.

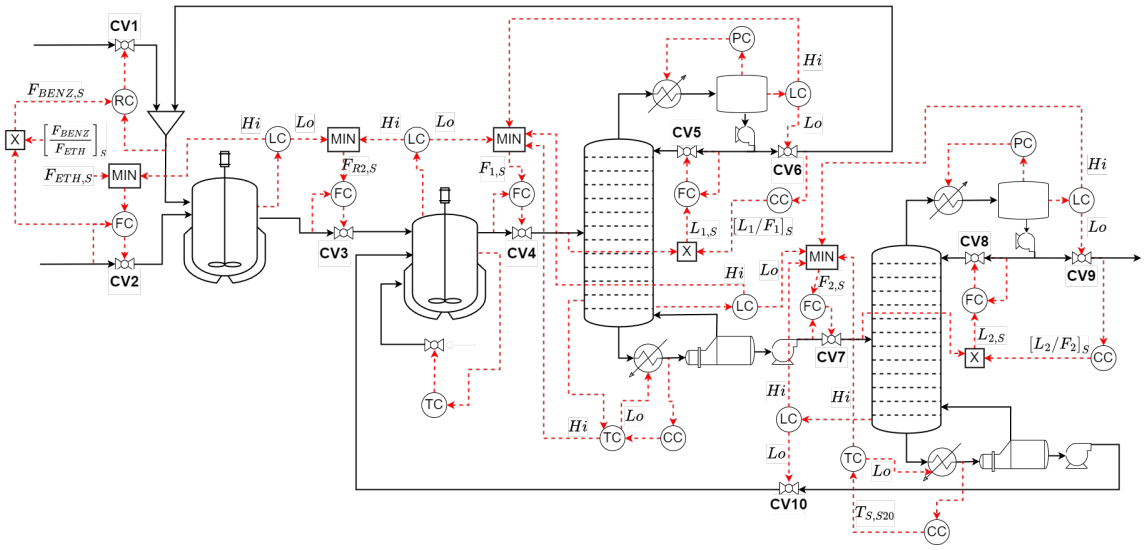

Figure 3.1 – Self-consistent bidirectional ethyl benzene plant.

In Section 2.1, it was demonstrated that a locally consistent distillation column can be efficiently regulated. The goal of this section is to do the same, but for the ethyl benzene plant. Using the same self-consistent logic as previously, we get the control structure shown in Figure 3.1. There are some remarks, however. The ratio controller to CV1 from CV2 does not have any feedback correction, so the plant may not be consistent in a long operation. The L-mode temperature controllers on both column also have H-mode overrides contrary to composition. As Luyben noted [11], operating a plant with on-line composition control can be expensive. In this case, composition control is optional, but stabilizing in some cases. It was experienced during some simulations that the bottoms impurity composition controller from column 1 introduced instabilities, so it was turned off for all simulations. Then, on column 1, we end up with a temperature-only controller on V. All composition controllers in the plant are using log transformed purity variables rather than absolute purity fractions.

Table 10 – Summary of events and constraint limit changes. Each row highlights the saturation of a manipulated variable and the corresponding new steady-state or setpoint values.

Time (h)	TPM (Controller)	Initial Value (F_S or F_T, kmol/hr)	New Value (F_S or F_T, kmol/hr)
1	Ethylene feed (CV2)	630.6	693.66 (+10%)
10	Column 2 feed valve (CV4)	1003.7	953.52 (-5%)
20	DEB recycle stream (CV10)	288.38	273.96 (-5%)
30	Benzene recycle stream (CV5)	982.00	933.85 (-5%)
40	Reactor 2 feed stream (CV3)	1532.67	1456.04 (-5%)

3.3 Simulation

Let us observe some points of interest in the simulation

1. The averaging effect of slow level controllers, which ultimately "smoothes" out the product flow. This also reduces economic loss.
2. The robustness of transfer between TPMs. There are MIN selectors on all valves, but only the MIN selectors on the column feeds are shown. The top graph is for column 1 and the bottoms is for column 2.
3. Despite the disturbances, the log transformed product purities (C2_CCLD.State in "product purity") remains constant.

Table 10 describe the simulation events in Figure 3.2. At t=1 hr, the ethylene feed is increased by 10%. When the feedrate increases (orange line in bottom graph) for ethylene, benzene also increases according to the ratio control $\left(\frac{F_{benz}}{F_{eth}}\right)_S$. Approximately 6 hours later, the first MV to saturate is the bottoms H-mode level controller for column 2 (C2_LCHB). This implies that a lot of DEB is begin produced with increased feed flow. The "slow" reaction is due to the high volumes in both reactors. The levels in Rx1 and Rx2 (see "levels overview") increase, but since the volume is so large in both reactors, it is not that noticeable.

Then, at t = 10 hrs, the column 2 feed valve is saturated by 5% (see the top "Select Min Feed Rate"). Other than reactor 1 reaching SP_H, this is quite uneventful. The ethylene feed is reduced so that excess benzene can react with DEB.

At t = 20 hrs, the DEB recycle stream flow is reduced by 5%, which limits the transalkylation between DEB and benzene. This reduces the EB production at "throughput". C2_LCHB becomes active due to increased production of DEB.

At t = 30 hrs, the benzene recycle stream is restricted by 5%. The benzene accumulation in the column 1 reflux drum is visible in the top "select min feed rate". C1_LCLB becomes active because the feedrate to column 1 is reduced by C1_LCHD. Then downstream flow decreases temporarily

until it reaches a steady-state.

Finally, at t = 40 hrs, the feed stream to reactor 2 becomes the bottleneck. We see the level in reactor 2 going down (see "levels overview"). Both C1_LCHB and C2_LCHB become active due to increased production of DEB. When both sump levels have gone down, the reactor 2 level controller becomes active again and the system reaches steady-state.

Figure 3.3 shows the feed (top) and product stream (bottom) during 3 different feed-disturbance scenarios. We introduce a 1, 2 and 4 hour feed disturbance (+10%). For the 1 hour disturbance run (blue line), we see that no H-mode controllers became active. This is visible by the smooth "normal-distribution" line. For the 2 hour feed disturbance, we see in Figure 3.4 that 'C1_LCHB' becomes active due to the sump level in column one being above SP_H for long enough. This is exasperated for the 4 hour disturbance case, where even 'C2_LCHB becomes active in Figure 3.5.

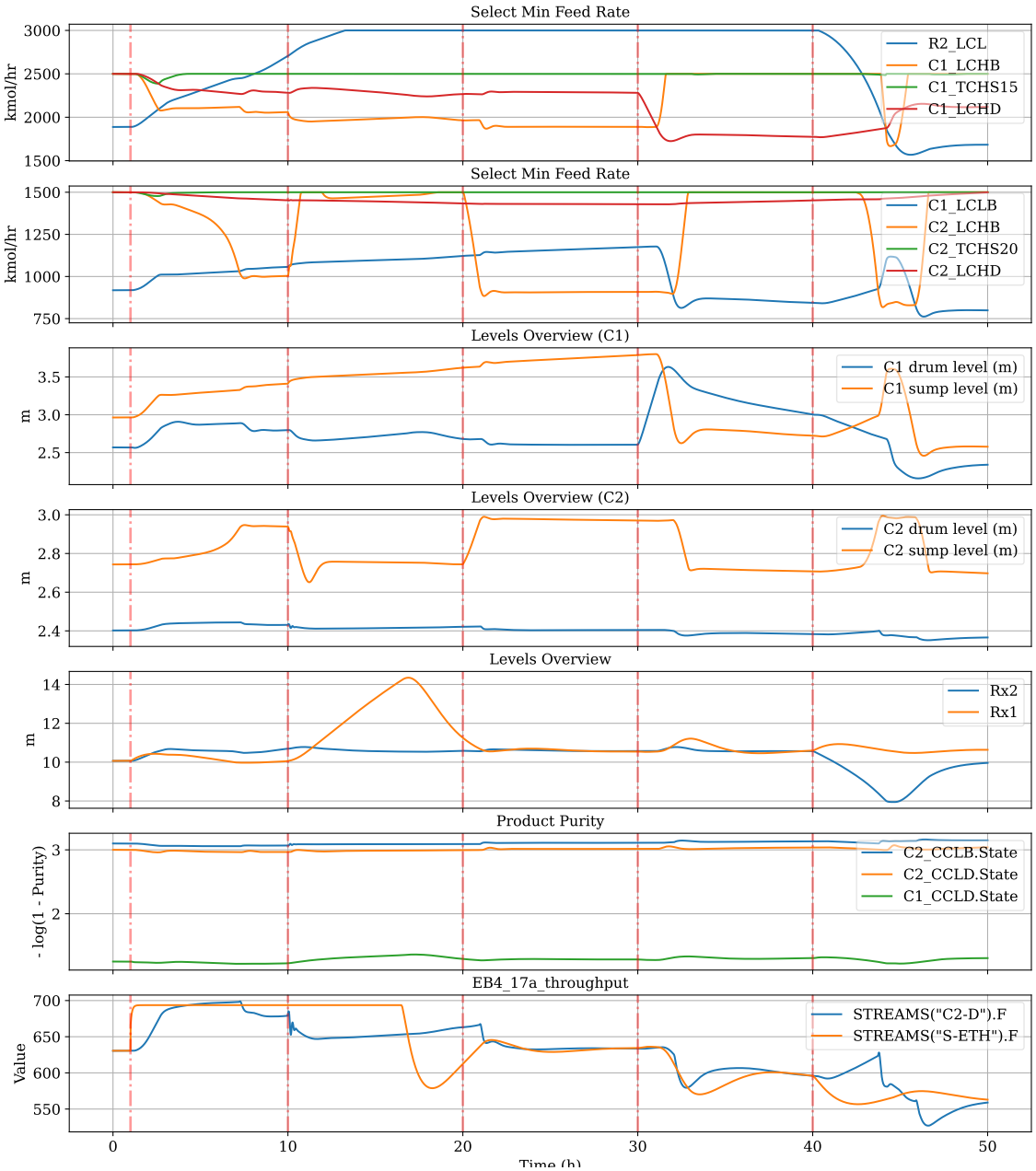

Figure 3.2 – EB: Full simulation following the bottleneck schedule in Table 10. The top "Select Min Feed Rate" is the feed of column 1 (C1). The other one is for column 2 (C2). Rx1 and Rx2 are reactor 1 and 2. The product purity is log transformed product impurity. C1_CCLD.State is the impurity (DEB) from column 1. The throughput lines in the bottoms graph describe molar flows in ethylene feed (orange line) and column 2 distillate (blue line; EB product).

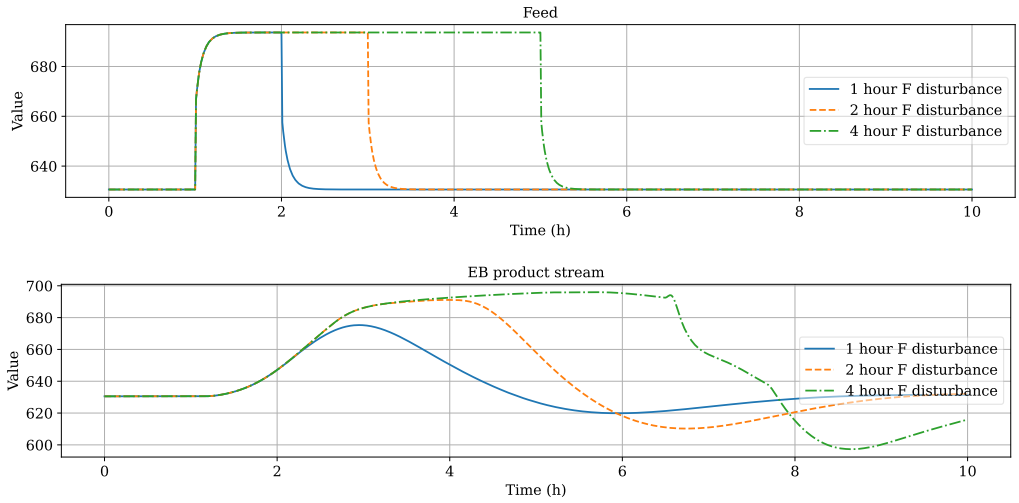

Figure 3.3 – Feed and product rate (all in kmol/hr) for a 10% disturbance in feed.

4 Discussion

In the introduction, we went sequentially through the process of "radiating" the TPM. This phenomenon has also been visible for both the simple distillation column and the ethyl benzene plant. When a bottleneck is reached and a controller "gives up", another controller takes over to "override" the the extensive in-flow rate to the throttled inventory. For open one-dimensional systems (i.e. flow does not recycle), this method is quite intuitive. However, when introducing recycle streams it was not certain whether the bidirectional method would work or not. We have seen in the EB plant that consistency rules hold either way.

For distillation columns, the relation between reboiler, reflux, levels and composition is vital. The first cases showcase how ratios between *extensive* flows stabilize the system. For columns specifically, one must increase the reflux (L) and boilup (V) proportionally to the feed (F). By using temperature as an intensive control variable to either the reflux or reboiler, we can use a feed-forward ratio controller to regulate the other flow. This, ideally, is total disturbance rejection.

There is, as mentioned, a trade-off between tight control and loose control. On one hand, tight control should be used for variables that otherwise have dynamic effects on the rest of the system. For example column temperature. We saw from BIDIR_1 when the reboiler duty was saturated that the temperature dropped significantly, which introduced dynamic effects everywhere in the system. Distillate flow decreases and feed is dumped into bottoms. Inventories on the other hand, and specifically levels, are not the same, since they share the same *intentive* variable no matter

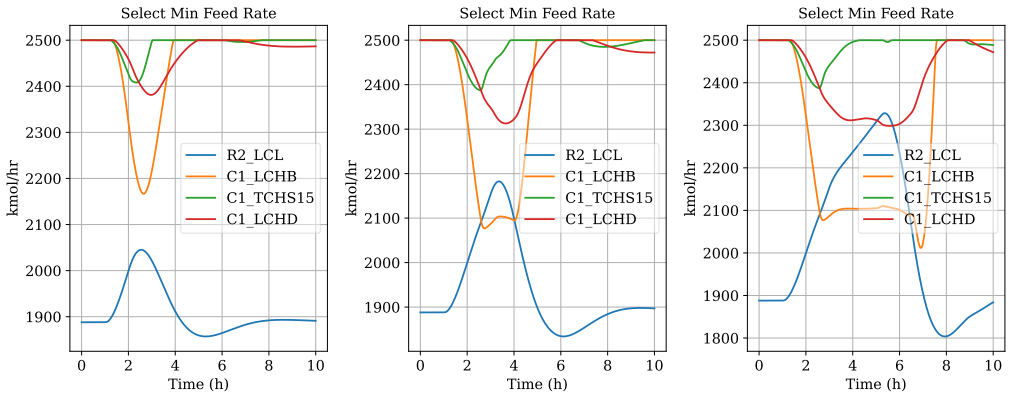

Figure 3.4 – MIN selector for column 1 during a 10% feed disturbance. To the left is for 1 hour feed disturbance. Middle is 2 hours and right is 4 hours.

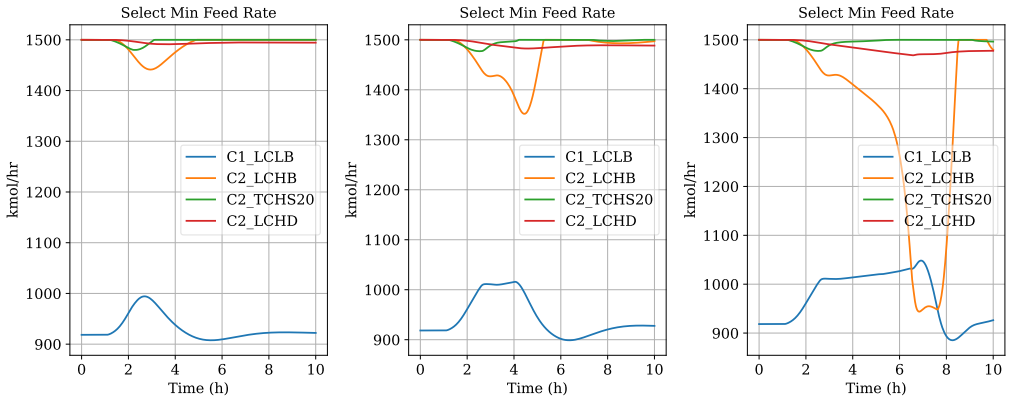

Figure 3.5 – MIN selector for column 2 during a 10% feed disturbance. To the left is for 1 hour feed disturbance. Middle is 2 hours and right is 4 hours.

how high or low the level is. Tanks are traditionally used as buffers for this reason. As shown in BIDIR_2 and the ethyl benzene plant, "loose control" was shown to be very promising. The system can not be too loose, though since we would end up with system-scale slow oscillations due to slow integrators. There is an optimum between "tight" and "loose" control that should allow for ideal average throughput.

Using the two additional (adaptive) tuning parameters Δu_T^* and Δy_S^*, this can likely be achieved.

Before, I was slightly mistaken when stating that bidirectional control can "solve" for maximum throughput. It would be a more correct statement to say that bidirectional control implemented in a correct way always will find the current bottleneck, and adjust all other *extensive* variables accordingly. The cost function in Equation 1.6a would be better to implement with an MPC, given that the MPC can model the system in question. The time it takes for piecewise radiation can be approximated to $T_{lag,i} = \theta_{T,i} + \tau_{y,i}$, where i is each operation. Say that the plant has to go through 4 TPM override operations to achieve steady-state. $\sum_i^N T_{lag,i}$ would suddenly depend on how tight the controllers are, and how big Δu_T^* and Δy_S^*. Then, intuition tells us that both of the prior variables should be as small as possible to reduce T_{lag}. For u_T^*, this is believed to be true, since we want the override to act as fast as possible when SP_H is reached, but not necessarily be too tight. Δy_S^* should for tightly controlled parameters also be small, but let us examine the extreme case.

What would happen if $\Delta y_S^* = 0$? In practice, it would be more like two L-controllers fighting for the same MV. It could resemble a MIMO system since there would be two or more MVs controlling the same CV at the same time. Essentially, each CV would on average have more than one MVs controlling it, and each MV would control more than one CV. However, unlike a regular MIMO where a scaled sum of transformed inputs would decide the CV magnitude, only a single input/setpoint through the MIN selector would decide the CV magnitude for a bidirectional plant with $\Delta y_S^* = 0$. Therefore, SP_H can not be equal SP_L, since that would imply that the controllers are competing constantly. While the H-mode controller for CV_γ is triggered yet inactive ($u_T^* > u_L$), we also know that the L-mode controller for CV_k is inactive. This means that CV_k is not controlled, and the system can become inconsistent. We should therefore treat Δy_S^* as a necessary buffer for H-mode controllers. On the other hand, what uses does a high Δy_S^* have? For level controllers, this means that the level becomes relatively high before the H-mode controller starts reacting. It may be better to have a moderate Δy_S^* instead, and rather choose "loose" tuning parameters for the controller. This would in practice achieve the same effect, except without an aggressive controller potentially causing system disturbances.

A possible modification for override control is implementing a model-based trajectory estimator that activates the H-mode controller pre-emptively to reduce θ_T (input tracking) or θ_0 (without input tracking). This effectively reduces delay, and may neglect it altogether. A drawback with estimators (Kalman filters etc.) are still the model inaccuracies, and possibly needless overrides, which may affect economic viability. Then another mode of operation could be a "multidirectional control", which effectively is a form of MPC. By weighting the overrides across several upstream MVs when SP_H is reached, the total lag T_{lag} will be distributed across several operations in parallel rather than many operations in series. This is a possibility for further study.

Now regarding the study question: "Given a consistent system, what is the ideal choice of bidirec-

tional tuning parameters to maximize and/or average out throughput?" It may not be a definite answer to the issue, but there should be an ideal set between "tight" and "loose" tuning of H-mode controllers that reaches nominal operating conditions as fast as possible. With loose tuning, it is possible to achieve no economic loss "on average" (oscillation), which in some cases may be desirable when the feed is inconsistent. Input u_T^* and setpoint Δy_S^* dead bands should be set to moderately small in order to reduce effective delay for override control.

As for the second study question: "How can control loops be arranged such that any disturbance or bottleneck in the system radiates away consistently?" the findings in this thesis are that achieving self-consistency for all inventories is likely the best course of action. This usually implies the "close-pairing" rules of thumb. The novel thought in this thesis is the idea that a TPM must be able to radiate in all directions. If not, the bottleneck will get "stuck" and the system becomes inconsistent due to saturated MVs. The strongest suit of bidirectional control is that when the system reaches steady-state, the system is also at max throughput given the active system constraints.

Conclusion

In this thesis, bidirectional control has been demonstrated as a robust method for controlling highly non-linear systems, such as distillation columns, and has shown great efficacy in managing the ethylbenzene plant. Its versatility suggests it could be applied to any process involving a series of inventories. For example, bidirectional control may have significant applications in wastewater treatment and municipal water management where bottlenecks are plenty. However, the intrinsic delay between control actions in bidirectional systems can pose certain challenges, particularly in processes requiring rapid response times.

1. **Fine-Tuning Δy_T^* for Tight Control**:
    - For controllers where precise regulation is critical, such as composition controllers, Δy_T^* should be minimized.
    - This reduces set-point offsets during overrides and shortens the effective delay before H-mode controllers are activated.
2. **"Averaging Control" for Non-Critical Variables**:
    - For control variables (y_k) where tight control is unnecessary (e.g., tank levels), larger Δy_T^* values can be used unless these variables significantly impact system stability or other critical states.
    - This introduces the concept of "averaging control," which can contribute to economic optimization.

3. **Minimizing Δu_T^* for Saturating Manipulated Variables**:
    - For manipulated variables (MVs) prone to saturation, Δu_T^* should generally be as small as possible.
    - Excessively small values may lead to erratic switching behavior in MIN selectors due to competition between H-mode controllers. In most cases, this is not a critical issue but should be carefully managed.
4. **Balancing Δy_T^* for Level Controllers**:
    - For level controllers, moderate Δy_T^* values are ideal. This balance:
        - Encourages averaging effects.
        - Reduces dynamic interactions between L-mode and H-mode level controllers.
        - Prevents competition between H-mode composition and level controllers in distillation columns.
    - Excessively high SP_H values for level controllers can unnecessarily increase effective delay without significant benefit.

References

[1] Sigurd Skogestad. "Advanced control using decomposition and simple elements". en. In: *Annual Reviews in Control* 56 (2023), p. 100903. ISSN: 13675788. DOI: 10.1016/j.arcontrol.2023.100903. URL: https://linkinghub.elsevier.com/retrieve/pii/S1367578823000676 (visited on 09/20/2024).

[2] Jingqing Han. "From PID to Active Disturbance Rejection Control". In: *IEEE Transactions on Industrial Electronics* 56.3 (Mar. 2009), pp. 900–906. ISSN: 0278-0046. DOI: 10.1109/TIE.2008.2011621. URL: http://ieeexplore.ieee.org/document/4796887/ (visited on 12/30/2024).

[3] Tore Hägglund and José Luis Guzmán. "Give us PID controllers and we can control the world". en. In: *IFAC-PapersOnLine* 58.7 (2024), pp. 103–108. ISSN: 24058963. DOI: 10.1016/j.ifacol.2024.08.018. URL: https://linkinghub.elsevier.com/retrieve/pii/S2405896324007316 (visited on 09/20/2024).

[4] Cristina Zotică, Krister Forsman, and Sigurd Skogestad. "Bidirectional inventory control with optimal use of intermediate storage". en. In: *Computers & Chemical Engineering* 159 (Mar. 2022), p. 107677. ISSN: 00981354. DOI: 10.1016/j.compchemeng.2022.107677. URL: https://linkinghub.elsevier.com/retrieve/pii/S0098135422000217 (visited on 12/30/2024).

[5] Randel M. Price, Philip R. Lyman, and Christos Georgakis. "Throughput Manipulation in Plantwide Control Structures". en. In: *Industrial & Engineering Chemistry Research* 33.5 (May 1994), pp. 1197–1207. ISSN: 0888-5885, 1520-5045. DOI: 10.1021/ie00029a016. URL: https://pubs.acs.org/doi/abs/10.1021/ie00029a016 (visited on 12/30/2024).

[6] Elvira Marie B. Aske. "Design of plantwide control systems with focus on maximizing throughput". Eng. PhD. Trondheim, 2009.

[7] Dale E. Seborg. *Process dynamics and control*. Fourth edition. Hoboken, NJ: Wiley, 2017. ISBN: 9781119285915.

[8] William L. Luyben. "Design and control of the ethyl benzene process". en. In: *AIChE Journal* 57.3 (Mar. 2011), pp. 655–670. ISSN: 0001-1541, 1547-5905. DOI: 10.1002/aic.12289. URL: https://aiche.onlinelibrary.wiley.com/doi/10.1002/aic.12289 (visited on 12/29/2024).

[9] Rahul Jagtap, Ashok S Pathak, and Nitin Kaistha. "Economic plantwide control of the ethyl benzene process". en. In: *AIChE Journal* 59.6 (2012), pp. 1996–2014. ISSN: 0001-1541, 1547-5905. DOI: 10.1002/aic.13964. URL: https://aiche.onlinelibrary.wiley.com/doi/10.1002/aic.13964 (visited on 09/20/2024).

[10] Sigurd Skogestad. "Simple analytic rules for model reduction and PID controller tuning". en. In: *Journal of Process Control* 13.4 (June 2003), pp. 291–309. ISSN: 09591524. DOI: 10.

1016/S0959-1524(02)00062-8. URL: https://linkinghub.elsevier.com/retrieve/pii/S0959152402000628 (visited on 12/31/2024).

[11] William L. Luyben. "Comparison of additive and multiplicative feedforward control". en. In: *Journal of Process Control* 111 (Mar. 2022), pp. 1–7. ISSN: 09591524. DOI: 10.1016/j.jprocont.2022.01.004. URL: https://linkinghub.elsevier.com/retrieve/pii/S095915242200004X (visited on 12/29/2024).

[12] William L. Luyben. "Corrigendum to "Comparison of additive and multiplicative feedforward control" [J. Process Control 111 (C) (2022) 1–7]". en. In: *Journal of Process Control* 113 (May 2022), pp. 96–100. ISSN: 09591524. DOI: 10.1016/j.jprocont.2022.03.012. URL: https://linkinghub.elsevier.com/retrieve/pii/S0959152422000506 (visited on 04/15/2024).

[13] William L. Luyben, ed. *Distillation Design and Control Using Aspen™ Simulation*. en. 1st ed. Wiley, Apr. 2013. ISBN: 9781118411438 9781118510193. DOI: 10.1002/9781118510193. URL: https://onlinelibrary.wiley.com/doi/book/10.1002/9781118510193 (visited on 04/14/2024).

[14] Thor Mejdell and Sigurd Skogestad. "Composition estimator in a pilot-plant distillation column using multiple temperatures". en. In: *Industrial & Engineering Chemistry Research* 30.12 (Dec. 1991), pp. 2555–2564. ISSN: 0888-5885, 1520-5045. DOI: 10.1021/ie00060a008. URL: https://pubs.acs.org/doi/abs/10.1021/ie00060a008 (visited on 12/25/2024).

Appendices

A Bidirectional Ethyl Benzene Plant

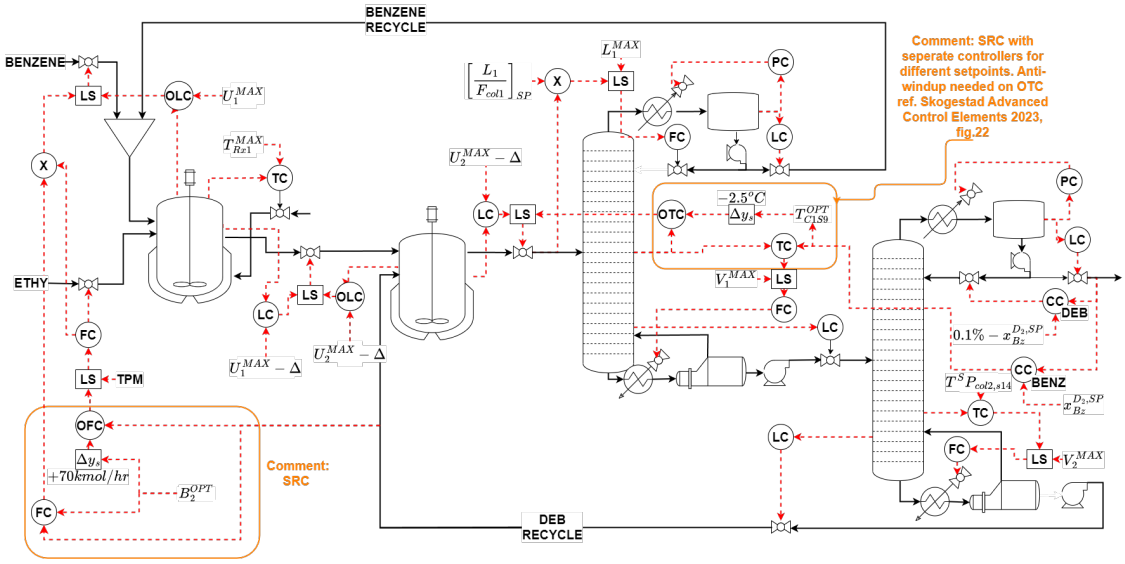

Figure A.1 – Bidirectional Control for an Ethyl Benzene Plant. Figure adapted from [9].

B Ethyl Benzene Plant Conditions

Table 11 – Reactor Parameters

Parameter	Reactor 1	Reactor 2
Type	Coil-cooled CSTR	Adiabatic CSTR
Operating Volume	200 m^3	200 m^3
Temperature	Controlled via cooling	Operates adiabatically
Reactants	Benzene and Ethylene	Benzene and DEB (Recycle Stream)
Key Reaction	$C_6H_6 + C_2H_4 \rightarrow C_8H_{10}$	$C_{10}H_{14} + C_6H_6 \rightarrow 2C_8H_{10}$
Purpose	Main alkylation reaction	Transalkylation to recycle DEB
Special Notes	Operated in excess benzene to suppress DEB formation	Recovers DEB through transalkylation

Table 12 – Column Parameters

Parameter	Column 1 (Recycle Column)	Column 2 (Product Column)
Trays	19	23
Purpose	Recover unreacted benzene (distillate)	Recover ethylbenzene as distillate, DEB as bottoms
Distillate Composition	High benzene	99.9 mol% ethylbenzene
Bottoms Composition	Ethylbenzene and DEB	Diethylbenzene (Recycle Stream)
Operating Pressure	Vacuum	Vacuum
Condenser Type	Water-cooled	Water-cooled
Special Notes	Avoid flooding; boilup constrained to 20% above base case	Maintain tight product purity control

C Ethyl Benzene Plant Column Temperature Profiles

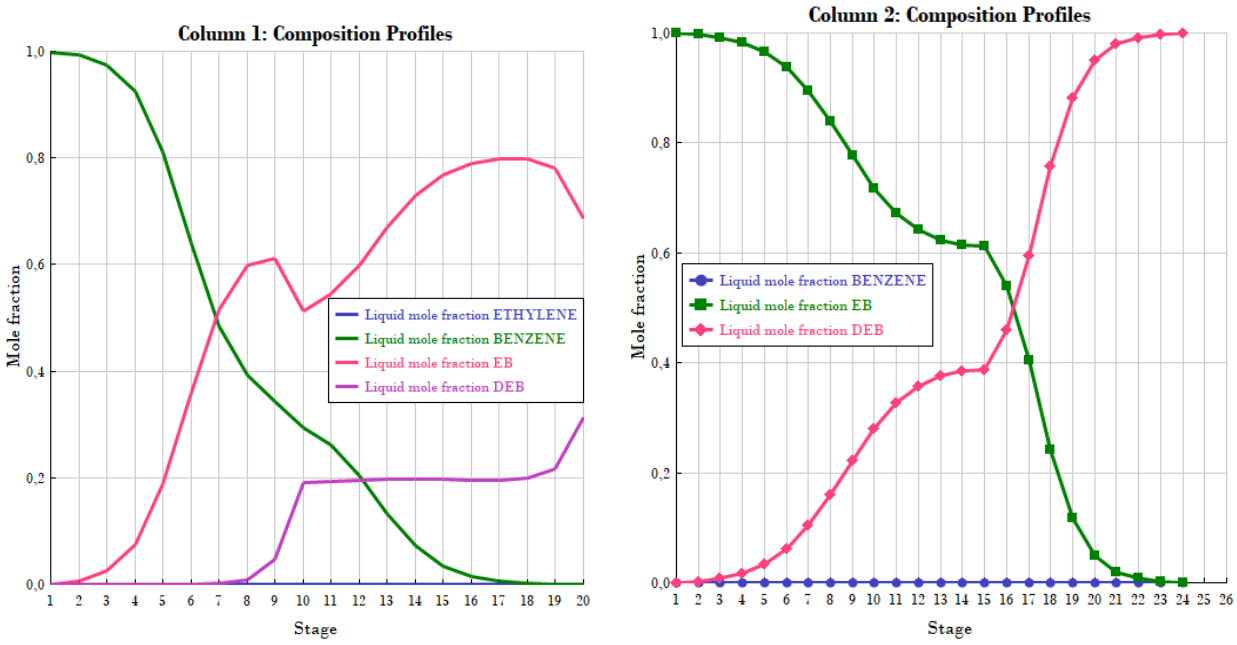

(a) (b)

Figure C.1 – Ethyl benzene plant distillation column composition profiles.
(a) Composition profile for column 1. At stage 1, pure benzene is recycled back to reactor 1.
(b) Composition profile for column 2. The feed from the bottom of column 2 (EB and DEB) are separated. The setpoint composition for both D and B is 0.999 (1.e3).

D Ethyl Benzene Controller Tuning

Table 13 – Controller parameter summary for the ethyl benzene plant in Figure 3.1. All temperature controllers have a lag of 1 minute and composition controllers have a 2 minute delay.

Controller	K_c	τ_I **(s)**	Δy^*	$u^*_{\mathbf{MAX}}$	**Special Notes**
R1_LCH	1	7200	0.5	-	High level in reactor 1
R1_LCL	-2	7200	-	-	Low level in reactor 1
R2_LCH	1	7200	0.5	-	High level in reactor 2
R2_LCL	-2	7200	-	-	Low level in reactor 2
R2_TC	5	360	-	-	Temperature control for reactor 2
C1_LCHB	4	3600	1.5	2500	High bottoms level in column 1
C1_LCHD	1	36000	1.5	2500	High distillate level in column 1
C1_LCLB	-1	9999999	-	-	Low bottoms level in column 1
C1_LCLD	1	9999999	-	-	Low distillate level in column 1
C1_PC	20	720	-	-	Pressure control in column 1
C1_TCLS15	-2	1200	-	-	Temperature control (stage 15, low)
C1_TCHS15	-10	36000	-0.5	2500	Temperature control (stage 15, high)
C1_CCB	-	-	-	-	Bottoms composition control
C1_CCLD	1	400000	-	-	Distillate composition control
C2_LCHD	0.5	3600	1.5	1500	High distillate level in column 2
C2_LCLD	10	999999	-	-	Low distillate level in column 2
C2_LCHB	10	430000	0.1	1500	High bottoms level in column 2
C2_LCLB	10	999999	-	-	Low bottoms level in column 2
C2_PC	20	720	-	-	Pressure control in column 2
C2_TCLS20	5	1200	-	-	Temperature control (stage 20, low)
C2_TCHS20	10	220000	-0.5	1500	Temperature control (stage 20, high)
C2_CCB	1	220000	-	-	Bottoms composition control
C2_CCLD	1	400000	-	-	Distillate composition control